Future Measurements of the Nucleon Elastic Electromagnetic Form Factors at Jefferson Lab

G.P. Gilfoyle

University of Richmond, Richmond, VA 23173

Outline

1. Scientific Motivation
2. Necessary Background
3. The Measurements
4. What we hope to learn.
5. Summary and Conclusions

Koutoubia Mosque

Scientific Motivation

- Nucleon elastic electromagnetic form factors (EEFFs) are fundamental quantities.
- At low Q^2 describe the distribution of charge and magnetization within the proton and neutron.
- At higher Q^2 reflect the quark and gluon structure of the nucleon.
- Provide rigorous testing ground for nuclear models and QCD.
- Needed for nuclear structure and parity violation experiments.

Scientific Motivation

- Nucleon elastic electromagnetic form factors (EEFFs) are fundamental quantities.
- At low Q^2 describe the distribution of charge and magnetization within the proton and neutron.
- At higher Q^2 reflect the quark and gluon structure of the nucleon.
- Provide rigorous testing ground for nuclear models and QCD.
- Needed for nuclear structure and parity violation experiments.

EEFFs have played an essential role in nuclear and nucleon structure for more than a half century.

Where We Are: the Last Decade.

- The ratio G_E^p/G_M^p from recoil polarization measurements diverged from previous Rosenbluth separations.
  - Two-photon exchange (TPE).
  - Effect of quark orbital angular momentum (OAM).
- High-precision, low-Q^2 results at Bates and JLab show clear deviations from the dipole (see Ron Gilman's talk).
- The neutron magnetic form factor G_M^n still follows the dipole form.
- High-Q^2 G_E^n opens the door to flavor decomposition

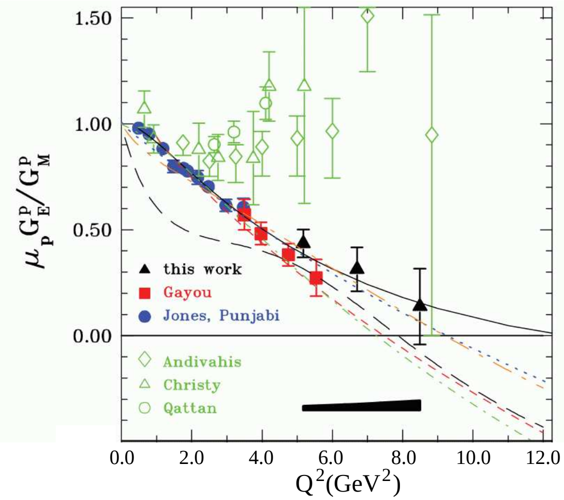

PRL **104**, 242301 (2010)

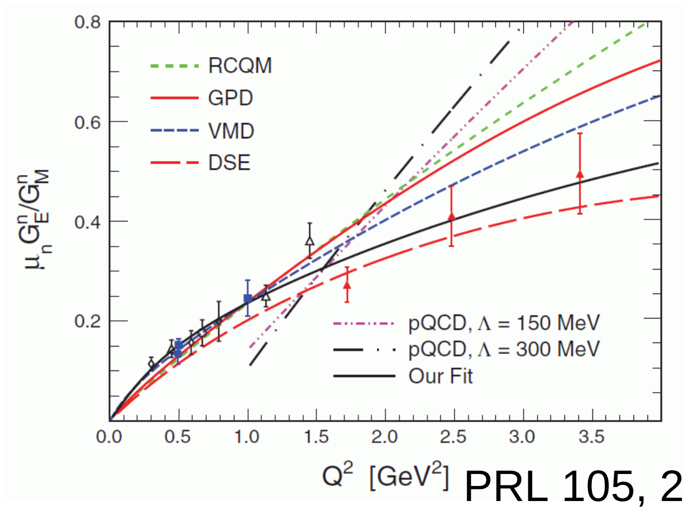

PRL 105, 262302

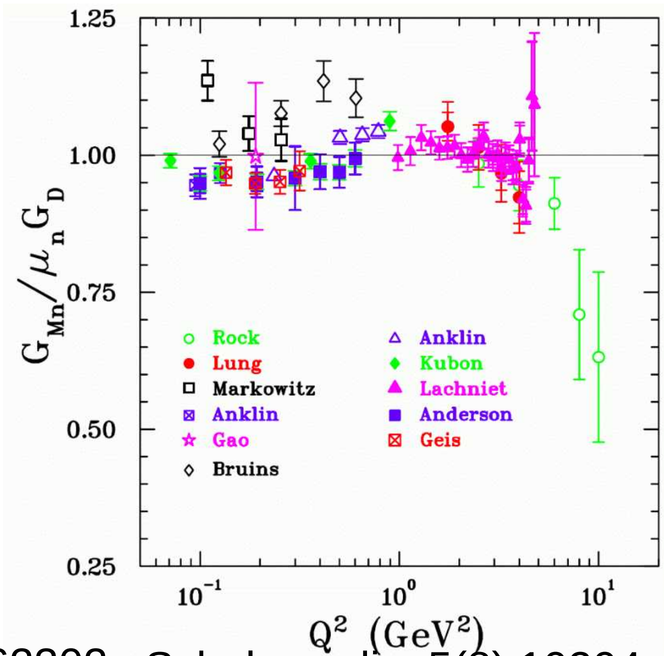

Scholarpedia, 5(8):10204

Where We Are: the Last Decade.

- The ratio G_E^p/G_M^p from recoil polarization measurements diverged from previous Rosenbluth separations.
  - Two-photon exchange (TPE).
  - Effect of quark orbital angular momentum (OAM).
- High-precision, low-Q^2 results at Bates and JLab show clear deviations from the dipole (see Ron Gilman's talk).
- The neutron magnetic form factor G_M^n still follows the dipole form.
- High-Q^2 G_E^n opens the door to flavor decomposition

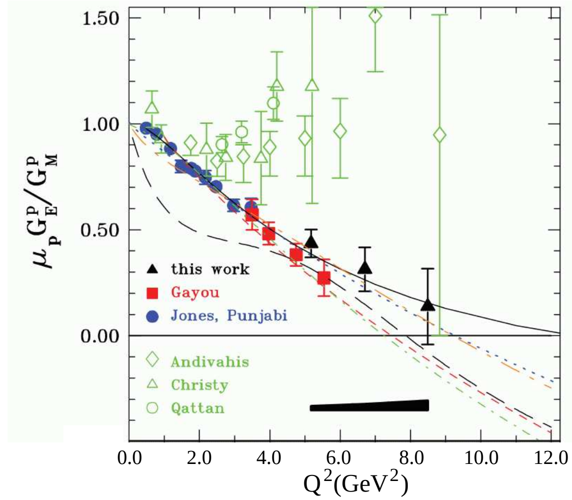

PRL **104**, 242301 (2010)

Advances driven by:

- high luminosity beams
- large acceptance detectors
- polarized beams, targets, detectors

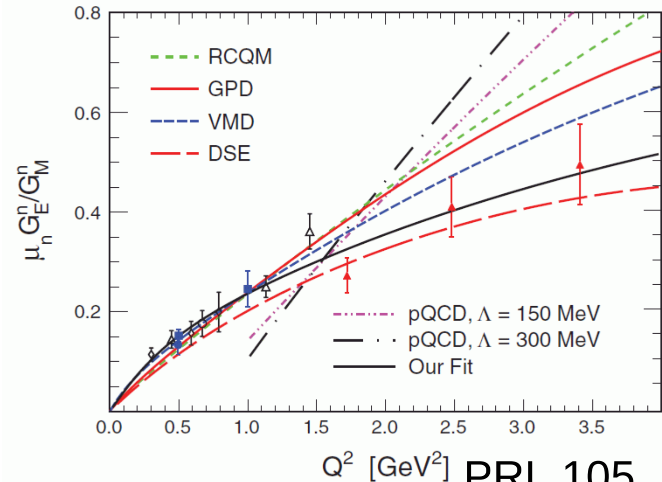

PRL 105, 262302

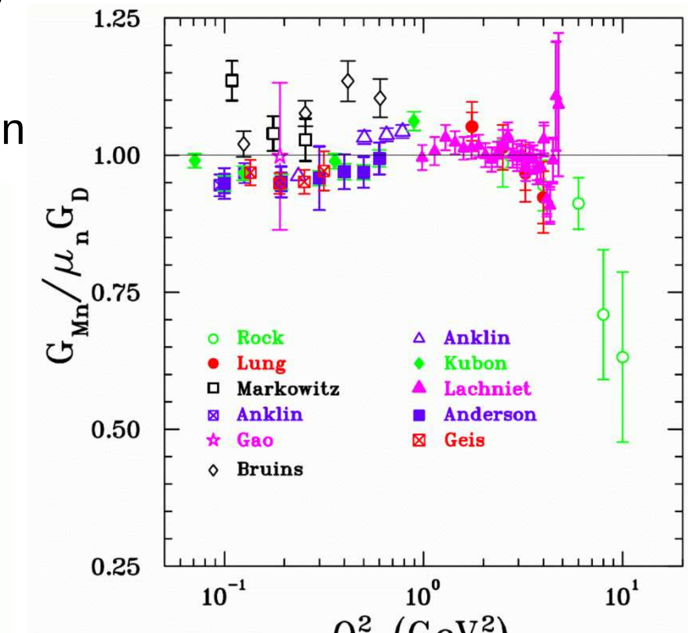

Scholarpedia, 5(8):10204

What We Hope to Learn.

- EEFFs are a major focus of the 12-GeV Upgrade at JLab.
- Reveal the internal landscape of the nucleon and nuclei.
- Test QCD and confinement in the non-perturbative regime.
- Map the transition from the hadronic picture to QCD.

What We Hope to Learn.

- EEFFs are a major focus of the 12-GeV Upgrade at JLab.
- Reveal the internal landscape of the nucleon and nuclei.
- Test QCD and confinement in the non-perturbative regime.
- Map the transition from the hadronic picture to QCD.

‘Recommendation I ...completion of the 12 GeV CEBAF Upgrade at Jefferson Lab.’

NSAC Long Range Plan (2007)

Some Necessary Background

- EEFFs cross section described with Dirac (F_1) and Pauli (F_2) form factors

$$\frac{d\sigma}{d\Omega} = \sigma_{Mott}\left[\left(F_1^2 + \kappa^2\tau F_2^2\right) + 2\tau\left(F_1 + \kappa F_2\right)^2 \tan^2\left(\frac{\theta_e}{2}\right)\right]$$

where

$$\sigma_{Mott} = \frac{\alpha^2 E' \cos^2(\frac{\theta_e}{2})}{4E^3 \sin^4(\frac{\theta_e}{2})}$$

and κ is the anomalous magnetic moment, E (E') is the incoming (outgoing) electron energy, θ is the scattered electron angle and $\tau = Q^2/4M^2$.

- For convenience use the Sachs form factors.

$$\frac{d\sigma}{d\Omega} = \sigma_{Mott}\left(\frac{(G_E^n)^2 + \tau(G_M^n)^2}{1+\tau} + 2\tau\tan^2\frac{\theta_e}{2}(G_M^n)^2\right)$$

where

$$G_E = F_1 - \tau F_2$$

$$G_M = F_1 + F_2$$

Some Necessary Background

- EEFFs cross section described with Dirac (F_1) and Pauli (F_2) form factors

$$\frac{d\sigma}{d\Omega} = \sigma_{Mott}\left[\left(F_1^2 + \kappa^2\tau F_2^2\right) + 2\tau\left(F_1 + \kappa F_2\right)^2 \tan^2\left(\frac{\theta_e}{2}\right)\right]$$

where

$$\sigma_{Mott} = \frac{\alpha^2 E' \cos^2(\frac{\theta_e}{2})}{4E^3 \sin^4(\frac{\theta_e}{2})}$$

and κ is the anomalous magnetic moment, E (E') is the incoming (outgoing) electron energy, θ is the scattered electron angle and $\tau = Q^2/4M^2$.

- For convenience use the Sachs form factors

Recall Ron Gilman's talk this morning.

where

$$G_E = F_1 - \tau F_2$$

$$G_M = F_1 + F_2$$

Some More Background - Interpreting the EEFFs

- At low momentum transfer ($Q^2 \ll M_N^2$) G_E and G_M are the Fourier transforms of the densities of charge and magnetization.

$$G_E(Q^2) = \int \rho(r) e^{-i\vec{q}\cdot\vec{r}} d^3r$$

where $\vec{q}$ is the 3-momentum transferred by the electron.

- At high Q^2 relativistic effects make the interpretation more interesting!

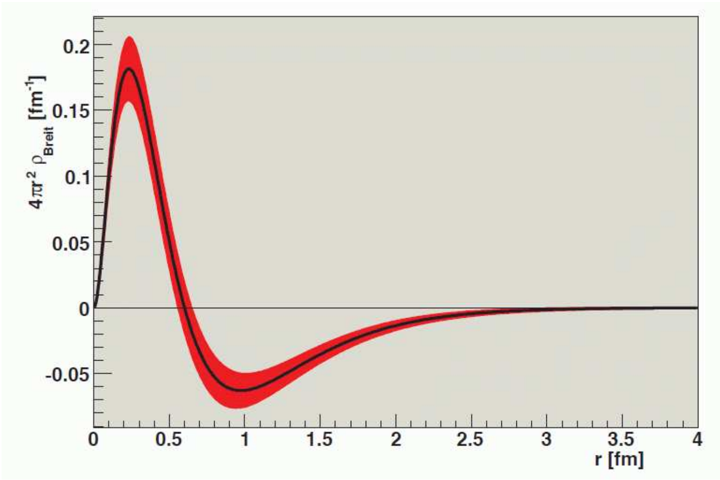

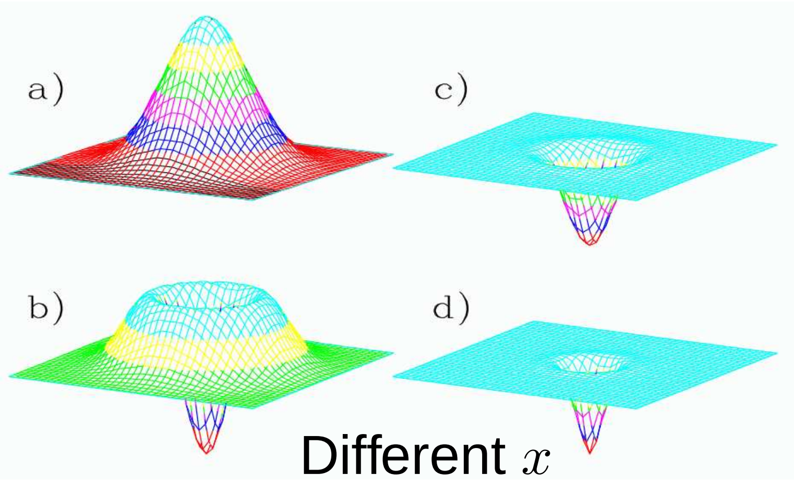

NSAC Long Range Plan

Arrington *et al.*, J.Phys.Conf.Ser. 299 (2011) 0120

Some More Background - Interpreting the EEFFs

- At low momentum transfer ($Q^2 \ll M_N^2$) G_E and G_M are the Fourier transforms of the densities of charge and magnetization.

$$G_E(Q^2) = \int \rho(r) e^{-i\vec{q}\cdot\vec{r}} d^3r$$

where $\vec{q}$ is the 3-momentum transferred by the electron.

- At high Q^2 relativistic effects make the interpretation more interesting!

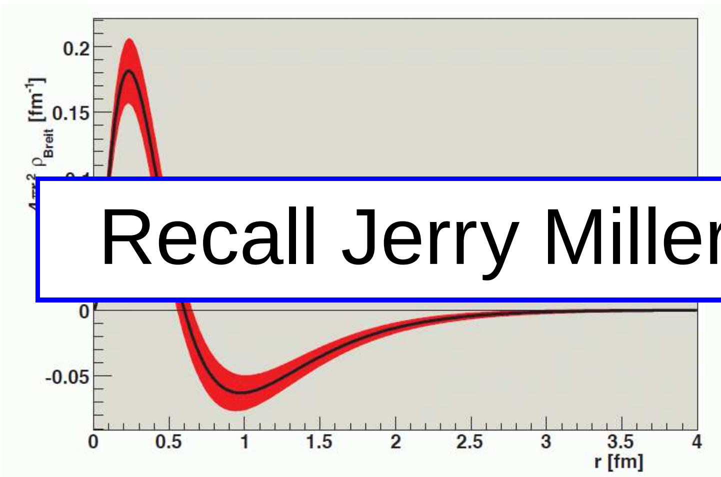

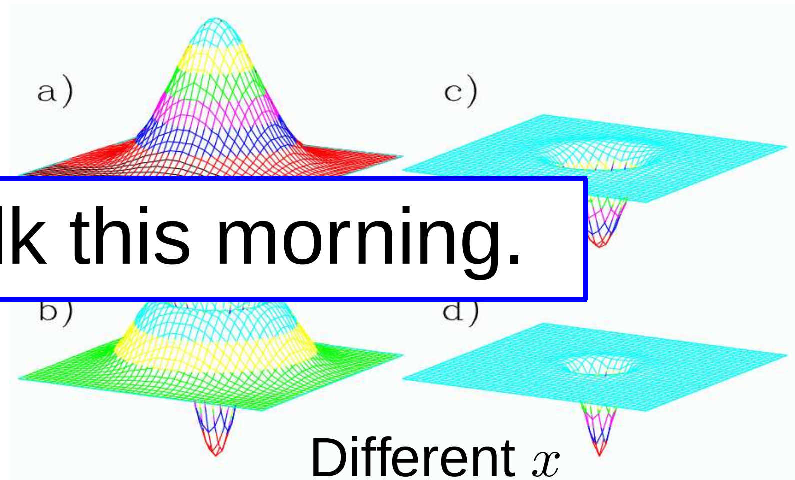

Recall Jerry Miller's talk this morning.

NSAC Long Range Plan

Arrington *et al.*, J.Phys.Conf.Ser. 299 (2011) 0120

Where We Are Going: New Experiments.

The JLab Lineup

Quantity	Method	Target	$Q^2(GeV^2)$	Hall	Beam Days
G_M^p	Elastic scattering	LH_2	$7-15.5$	A	24
G_E^p/G_M^p	Polarization transfer	LH_2	$5-12$	A	45
G_M^n	$E-p/e-n$ ratio	LD_2-LH_2	$3.5-13.0$	B	30
G_M^n	$E-p/e-n$ ratio	LD_2, LH_2	$3.5-13.5$	A	25
G_E^n/G_M^n	Double polarization asymmetry	polarized ^{3}He	$5-8$	A	50
G_E^n/G_M^n	Polarization transfer	LD_2	$4-7$	C	50

PAC approval for 224 days of running in the first five years.

Jefferson Lab

How We Will Get There: Jefferson Lab.

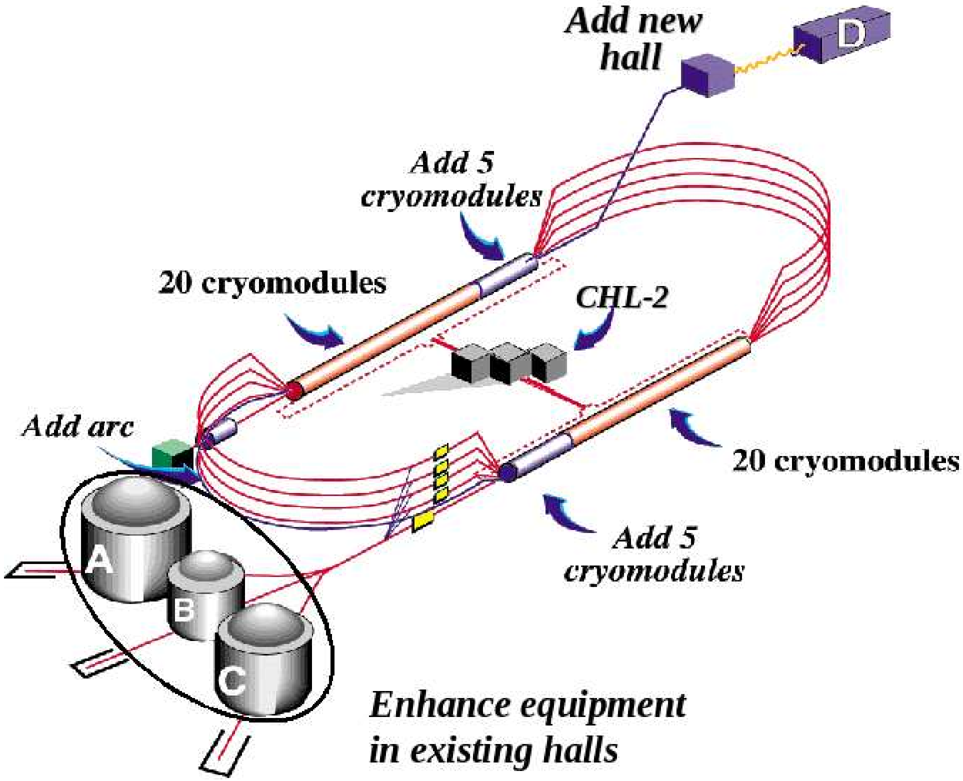

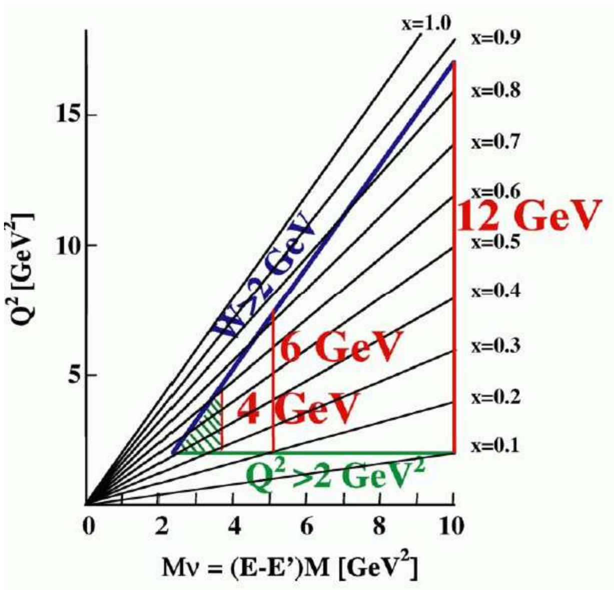

Continuous Electron Beam Accelerator Facility (CEBAF)

- Superconducting Electron Accelerator (currently 338 cavities), 100% duty cycle.
- $E_{max} = 11\ \mathrm{GeV}$ (Halls A, B, and C) and $12\ \mathrm{GeV}$ (Hall D), $\Delta E/E \approx 2 \times 10^{-4}$, $I_{summed} \approx 90\ \mu A$, $P_e \geq 80\%$.

How We Will Get There: Jefferson Lab.

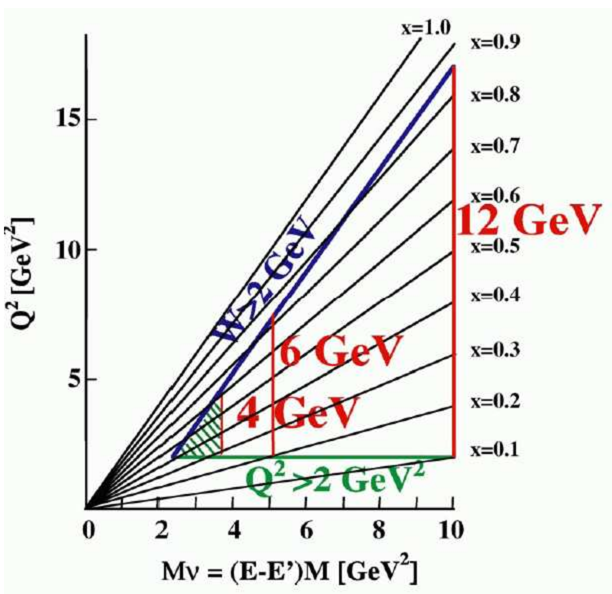

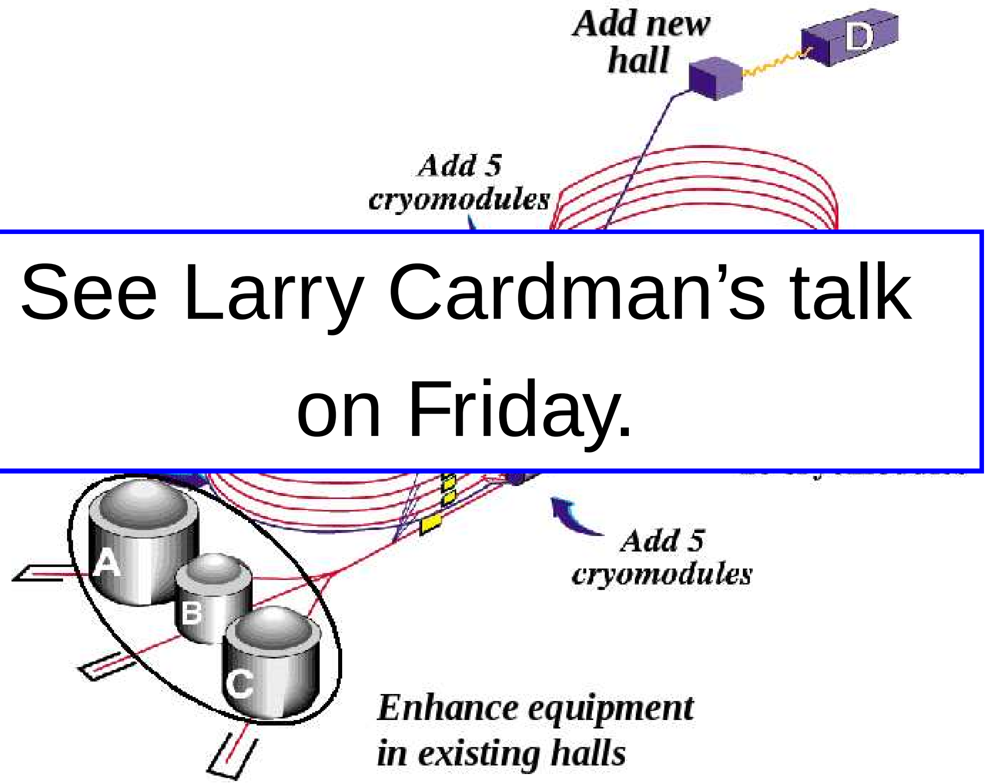

See Larry Cardman's talk on Friday.

Continuous Electron Beam Accelerator Facility (CEBAF)

- Superconducting Electron Accelerator (currently 338 cavities), 100% duty cycle.
- $E_{max} = 11$ GeV (Halls A, B, and C) and 12 GeV (Hall D), $\Delta E/E \approx 2 \times 10^{-4}$, $I_{summed} \approx 90\ \mu A$, $P_e \geq 80\%$.

The Experiment - New Detectors

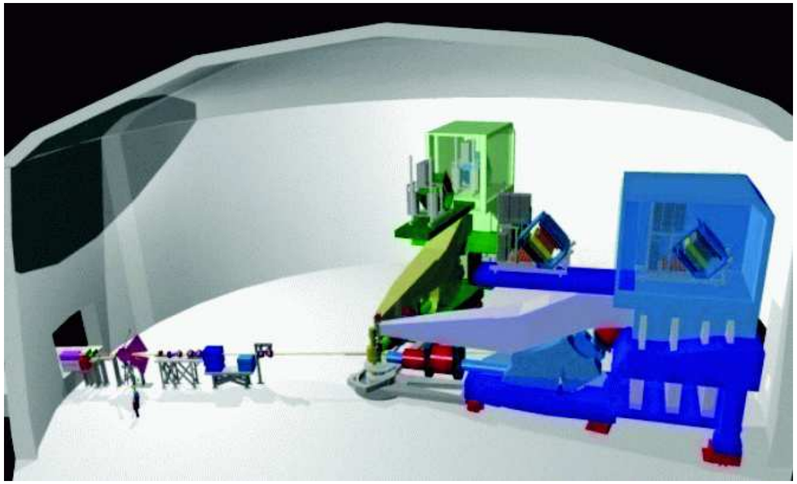

Hall A - High Resolution Spectrometer (HRS) pair, BigBite, neutron detector, and specialized installation experiments.

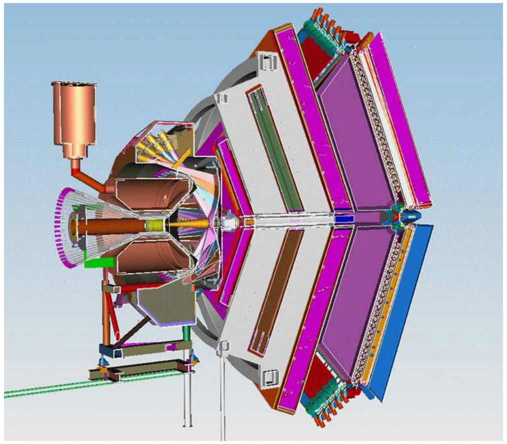

Hall B - CLAS12 large acceptance spectrometer operating at high luminosity with toroid (forward detector) and solenoid (central detector).

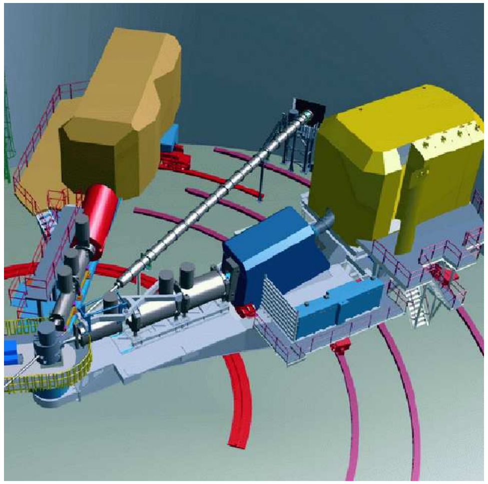

Hall C - New Super High Momentum Spectrometer to be used with the existing High Momentum Spectrometer.

Hall D - A new large acceptance detector based on a solenoid magnet for photon beam experiments is under construction.

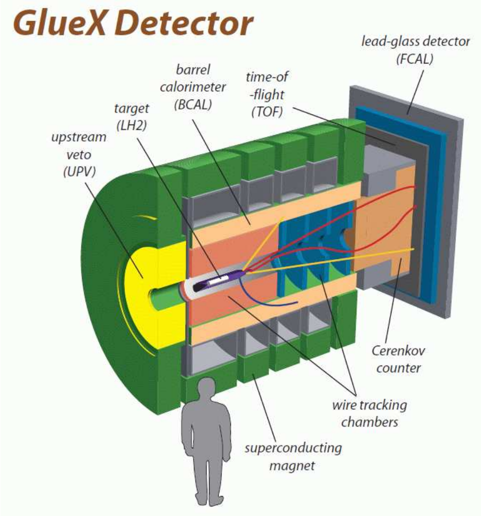

Proton Magnetic Form Factor - G_M^p

- E12-07-108 in Hall A (Gilad, Moffitt, Wojtsekhowski, Arrington).
- Precise measurement of ep elastic cross section and extract G_M^p.
- Both HRSs in electron mode.
- Beamtime: 24 days.
- $\mathrm{Q}^2 = 7.0-15.5\,\mathrm{GeV}^2$ ($1.0,\ 1.5\,\mathrm{GeV}^2$ steps).
- Significant reduction in uncertainties:

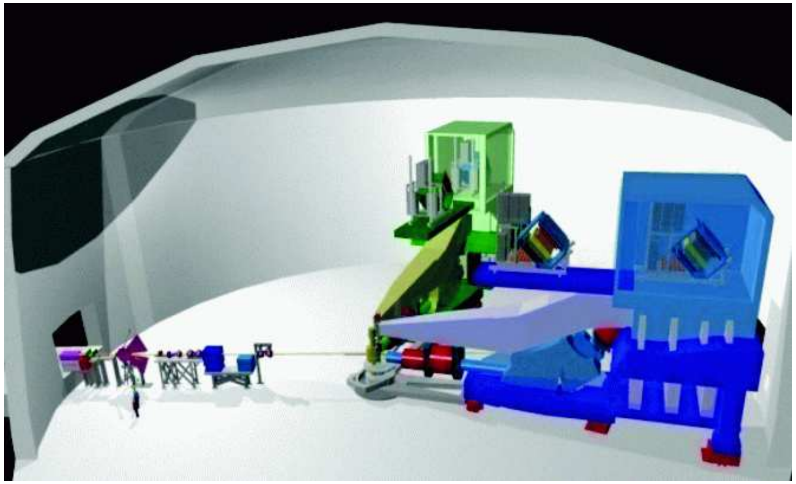

	$d\sigma/d\Omega$	G_M^p
Point-to-Point	1.0-1.3	0.5-0.6
Normalization	1.0-1.3	0.5-0.6
Theory	1.0-2.0	0.5-1.0

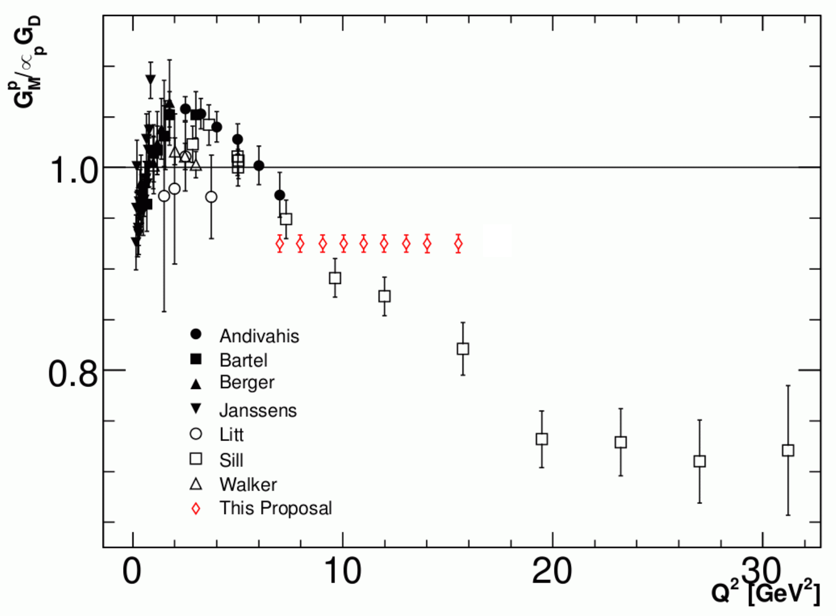

- Two-Photon Exchange is a major source of uncertainty → vary ϵ to constrain.
- Sets the scale of other EEFFs.

Proton Form Factor Ratio G_E^p/G_M^p

- E12-07-109 (GEp(5)) in Hall A (Brash, Jones, Perdrisat, Pentchev, Cisbani, Punjabi, Khandaker, Wojtsekhowski).
- Polarization transfer using $\mathrm{H}(\vec{e}, e'\vec{p})$:

$$\frac{G_E^p}{G_M^p} = -\frac{P_t}{P_l}\frac{E+E'}{2M}\tan\left(\frac{\theta_e}{2}\right)$$

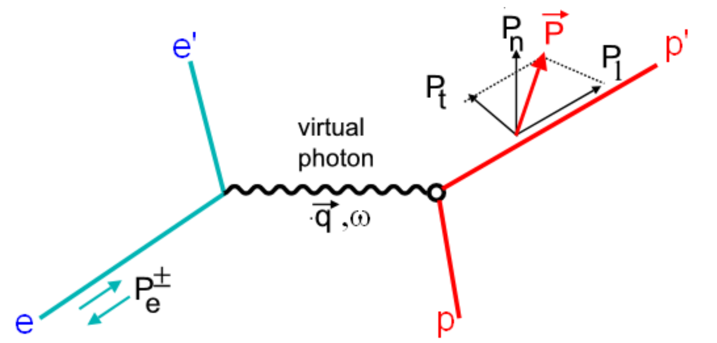

- Electron arm: EM calorimeter (BigCal).
- Proton arm: new, large-acceptance magnetic spectrometer (SBS) with double polarimeter, and hadron calorimeter.
- Beamtime: 45 days.
- Kinematics and Uncertainties:

Q^2 (GeV^2)	5.0	8.0	12.0
$\Delta[\mu G_E/G_m]$	0.025	0.031	0.069

- Combined with GEp(4).

Proton Form Factor Ratio G_E^p/G_M^p

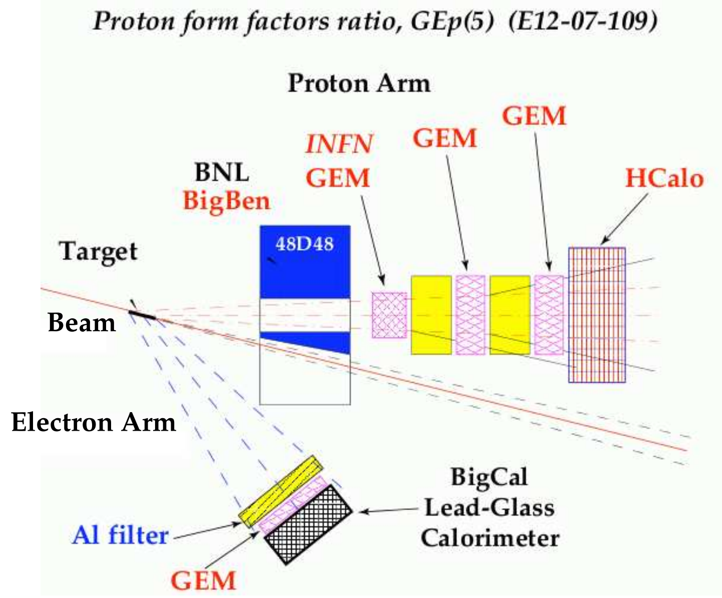

- E12-07-109 (GEp(5)) in Hall A (Brash, Jones, Perdrisat, Pentchev, Cisbani, Punjabi, Khandaker, Wojtsekhowski).
- Polarization transfer using $\mathrm{H}(\vec{e}, e'\vec{p})$:

$$\frac{G_E^p}{G_M^p} = -\frac{P_t}{P_l}\frac{E+E'}{2M}\tan\left(\frac{\theta_e}{2}\right)$$

- Electron arm: EM calorimeter (BigCal).
- Proton arm: new, large-acceptance magnetic spectrometer (SBS) with double polarimeter, and hadron calorimeter.
- Beamtime: 45 days.
- Kinematics and Uncertainties:

Q^2 (GeV^2)	5.0	8.0	12.0
$\Delta[\mu G_E/G_m]$	0.025	0.031	0.069

- Combined with GEp(4).

Proton Form Factor Ratio G_E^p/G_M^p

- E12-07-109 (GEp(5)) in Hall A (Brash, Jones, Perdrisat, Pentchev, Cisbani, Punjabi, Khandaker, Wojtsekhowski).
- Polarization transfer using $\mathrm{H}(\vec{e}, e'\vec{p})$:

$$\frac{G_E^p}{G_M^p} = -\frac{P_t}{P_l}\frac{E+E'}{2M}\tan\left(\frac{\theta_e}{2}\right)$$

- Electron arm: EM calorimeter (BigCal).
- Proton arm: new, large-acceptance magnetic spectrometer (SBS) with double polarimeter, and hadron calorimeter.
- Beamtime: 45 days.
- Kinematics and Uncertainties:

Q^2 (GeV^2)	5.0	8.0	12.0
$\Delta[\mu G_E/G_m]$	0.025	0.031	0.069

- Combined with GEp(4).

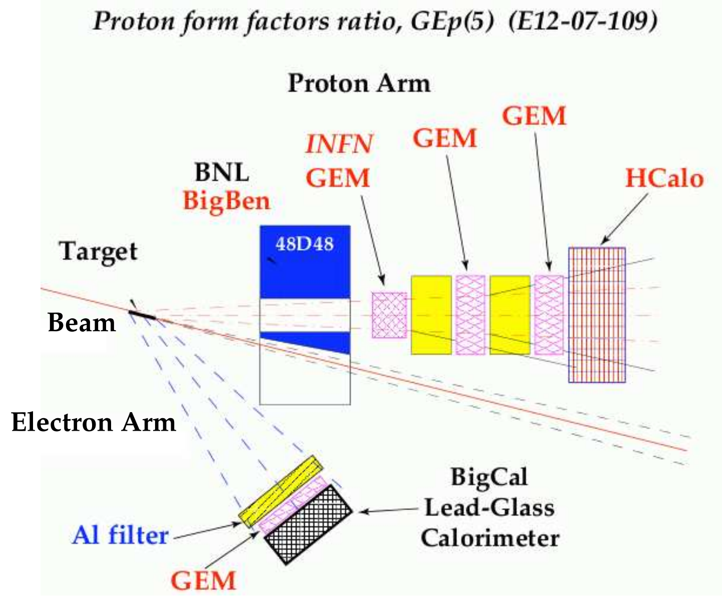

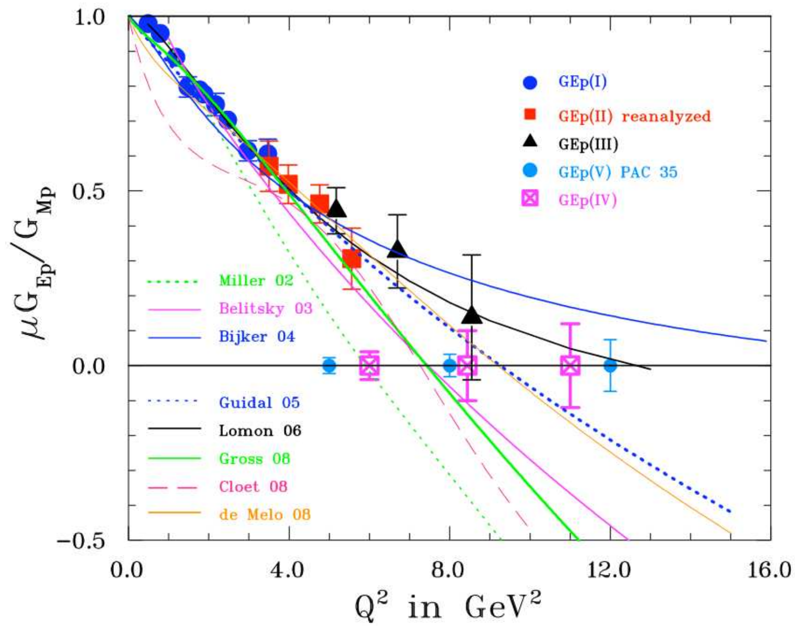

Neutron Magnetic Form Factor G_M^n - 1

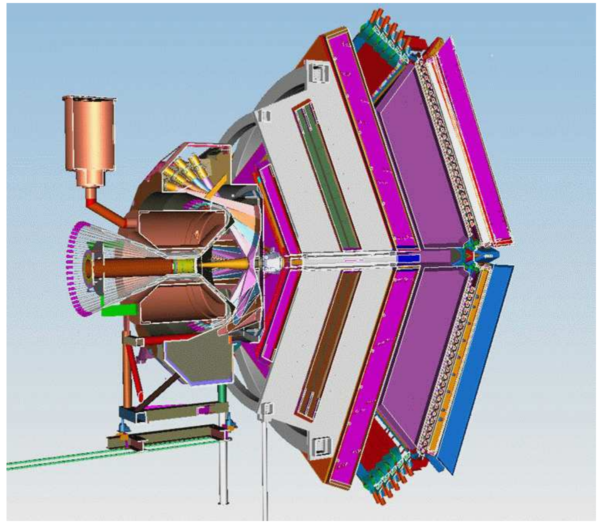

- E12-07-104 in Hall B (Gilfoyle, Hafidi, Brooks).
- Ratio Method on Deuterium ($^2\mathrm{H}(e,e'p)n$ and $^2\mathrm{H}(e,e'n)p$):

$$R = \frac{\frac{d\sigma}{d\Omega}[^2\mathrm{H}(e,e'n)_{QE}]}{\frac{d\sigma}{d\Omega}[^2\mathrm{H}(e,e'p)_{QE}]}$$

$$= a \times \frac{\sigma_{Mott}\left(\frac{(G_E^n)^2+\tau(G_M^n)^2}{1+\tau}+2\tau\tan^2\frac{\theta_e}{2}(G_M^n)^2\right)}{\frac{d\sigma}{d\Omega}[^1\mathrm{H}(e,e')p]}$$

where a is nuclear correction.

- Precise neutron detection efficiency needed to keep systematics low.
  - tagged neutrons from $p(e,e'\pi^+n)$.
  - Dual $LD_2 - LH_2$ target for *in situ* calibrations.

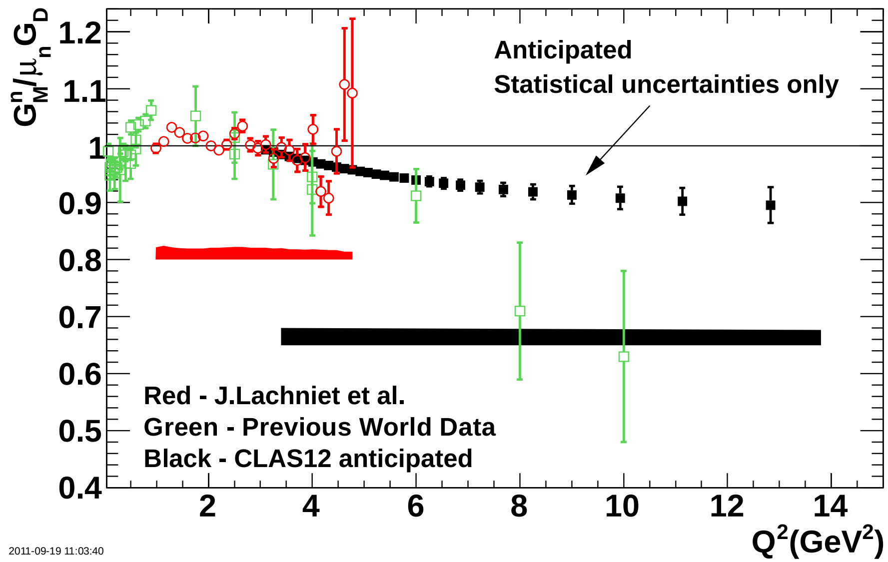

- Kinematics: $\mathrm{Q}^2 = 3.5 - 13.0\ (\mathrm{GeV/c})^2$.
- Beamtime: 30 days.
- Systematic uncertainties less than 2.5% across full Q^2 range.

Neutron Magnetic Form Factor G_M^n - 2

- E12-09-019 in Hall A (Quinn, Wojtsekhowski, Gilman).
- Ratio Method on Deuterium as in Hall B:

$$R = \frac{\frac{d\sigma}{d\Omega}[^2\mathrm{H}(e,e'n)_{QE}]}{\frac{d\sigma}{d\Omega}[^2\mathrm{H}(e,e'p)_{QE}]}$$

- Electron arm: BigBite spectrometer.
- Hadron arm: hadron calorimeter (HCal).
- Neutron detection efficiency:
  - Use $p(\gamma,\pi^+)n$ for tagged neutrons.
  - End-point method.
- Kinematics: $\mathrm{Q}^2 = 3.5 - 13.5\ (\mathrm{GeV/c})^2$.
- Beamtime: 25 days.
- Systematic uncertainties $< 2.1\%$.
- Two G_M^n measurements 'allow a better control for the systematic error' (PAC34).

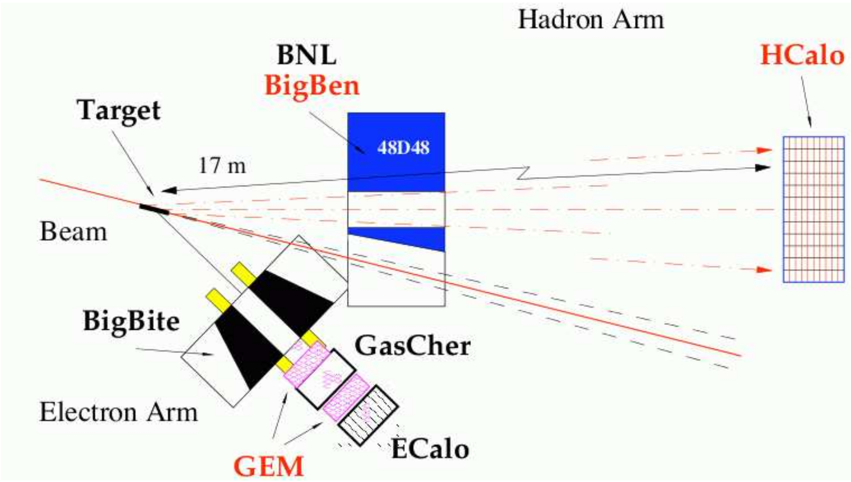

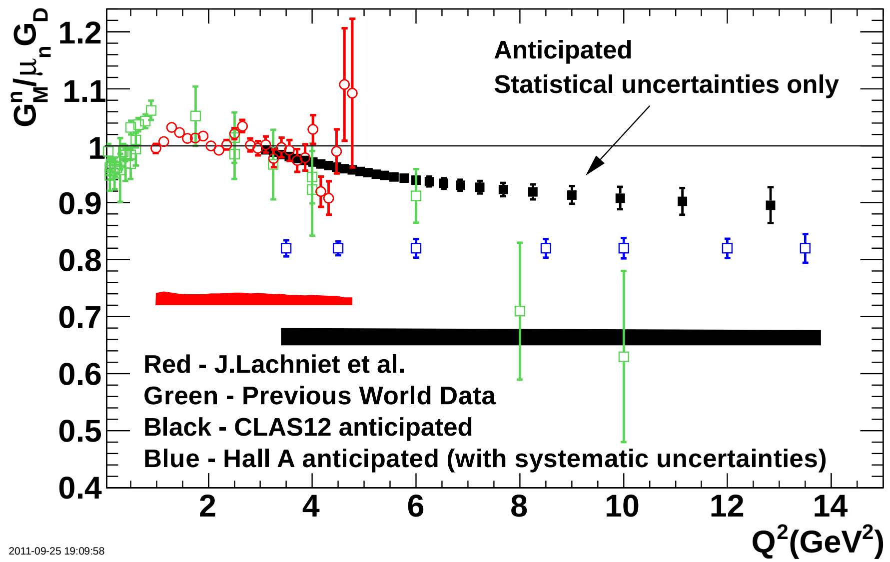

Neutron Magnetic Form Factor G_M^n - 2

- E12-09-019 in Hall A (Quinn, Wojtsekhowski, Gilman).
- Ratio Method on Deuterium as in Hall B:

$$R = \frac{\frac{d\sigma}{d\Omega}[^2\mathrm{H}(e,e'n)_{QE}]}{\frac{d\sigma}{d\Omega}[^2\mathrm{H}(e,e'p)_{QE}]}$$

- Electron arm: BigBite spectrometer.
- Hadron arm: hadron calorimeter (HCal).
- Neutron detection efficiency:
  - Use $p(\gamma,\pi^+)n$ for tagged neutrons.
  - End-point method.
- Kinematics: $\mathrm{Q}^2 = 3.5 - 13.5\ (\mathrm{GeV/c})^2$.
- Beamtime: 25 days.
- Systematic uncertainties $< 2.1\%$.
- Two G_M^n measurements 'allow a better control for the systematic error' (PAC34).

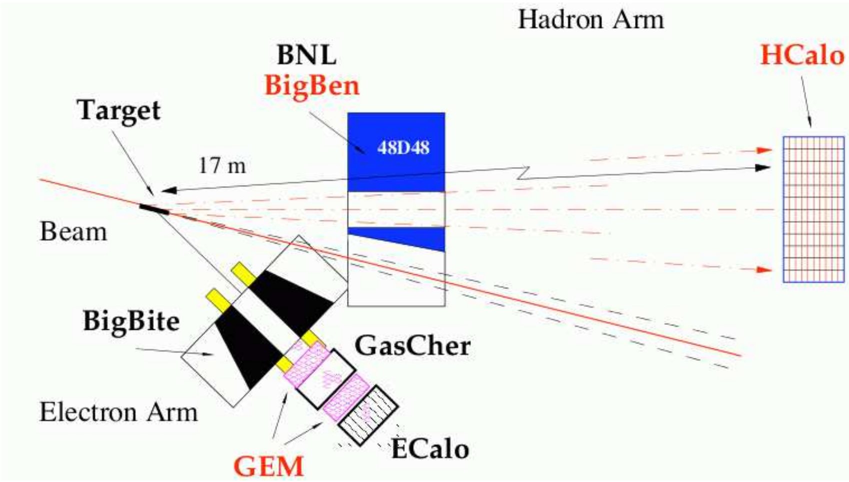

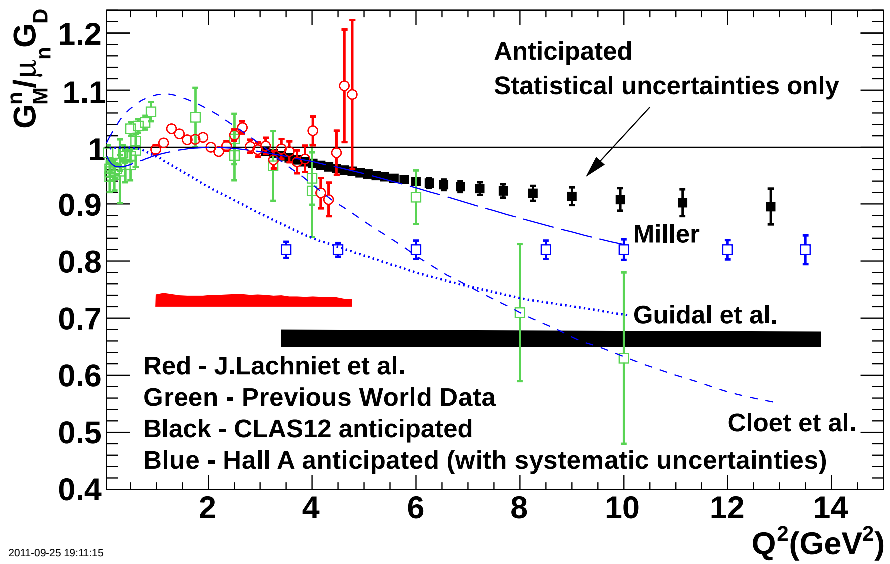

Neutron Form Factor Ratio G_E^n/G_M^n - 1

- E12-09-016 in Hall A (Cates, Wojtsekhowski, Riordan).
- Double Polarization Asymmetry: Get A_{en}^V from $^3\vec{\mathrm{He}}(\vec{e}, e'n)pp$.
- Longitudinally polarized electron beam.
- $^3\mathrm{He}$ target polarized perpendicular to the momentum transfer.
- Electron arm: BigBite spectrometer.
- Neutron arm: hadron calorimeter HCal (overlap with GEp(5) and Hall A G_M^n).
- Beamtime: 50 days.
- Kinematics and Uncertainties:

Q^2 (GeV^2)	5.0	6.8	8.0
$\Delta\left[\frac{\mu G_E}{G_M}\right]_{stat}$	0.027	0.022	0.032
$\Delta\left[\frac{\mu G_E}{G_M}\right]_{syst}$	0.018	0.021	0.013

$$A_{en}^V = \frac{-2\sqrt{\tau(\tau+1)}\tan(\theta_e/2)\cos\phi^*\sin\theta^* G_E^n/G_M^n}{(G_E^n/G_M^n)^2+\tau/\epsilon} + \frac{-2\tau\sqrt{1+\tau+(\tau+1)^2\tan^2(\theta_e/2)}\tan(\theta_e/2)\cos\theta^*}{(G_E^n/G_M^n)^2+\tau/\epsilon}$$

where $\epsilon = 1/\left(1+2(1+\tau)\tan^2(\frac{\theta_e}{2})\right)$

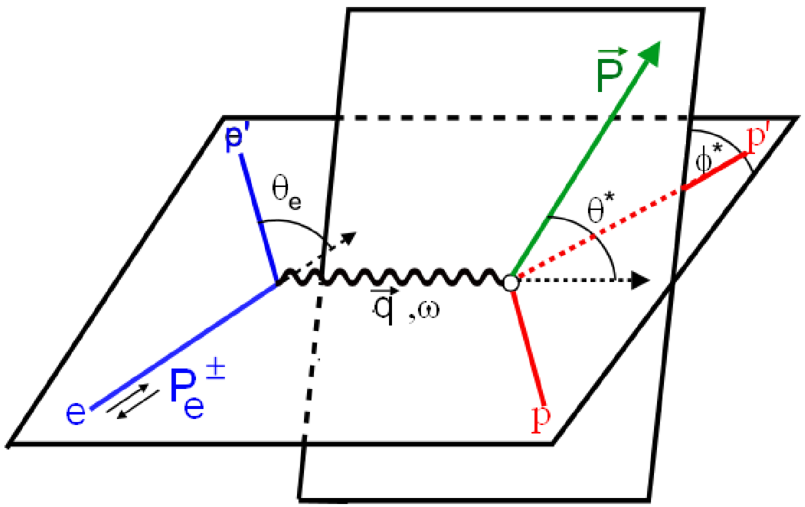

Neutron Form Factor Ratio G_E^n/G_M^n - 1

- E12-09-016 in Hall A (Cates, Wojtsekhowski, Riordan).
- Double Polarization Asymmetry: Get A_{en}^V from $^3\vec{\mathrm{He}}(\vec{e}, e'n)pp$.
- Longitudinally polarized electron beam.
- $^3\mathrm{He}$ target polarized perpendicular to the momentum transfer.
- Electron arm: BigBite spectrometer.
- Neutron arm: hadron calorimeter HCal (overlap with GEp(5) and Hall A G_M^n).
- Beamtime: 50 days.
- Kinematics and Uncertainties:

$\mathrm{Q}^2\ (\mathrm{GeV}^2)$	5.0	6.8	8.0
$\Delta\left[\frac{\mu G_E}{G_M}\right]_{stat}$	0.027	0.022	0.032
$\Delta\left[\frac{\mu G_E}{G_M}\right]_{syst}$	0.018	0.021	0.013

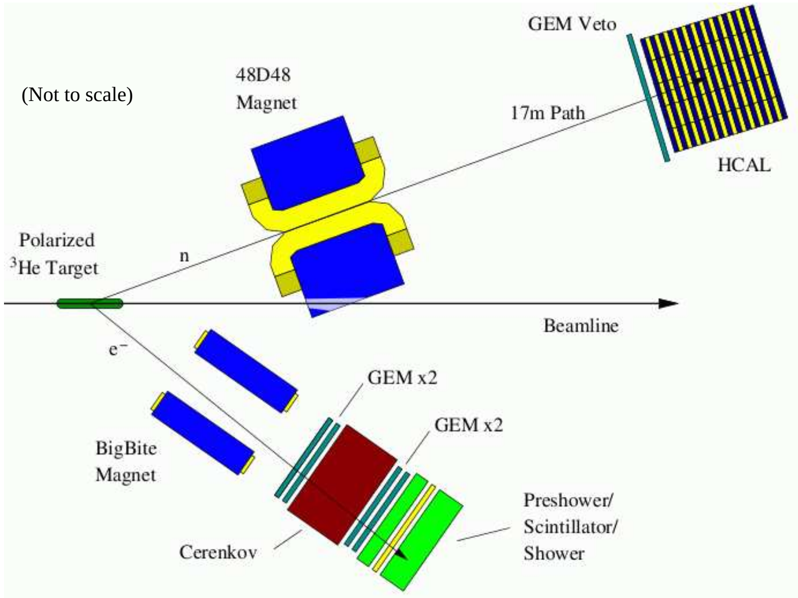

Neutron Form Factor Ratio G_E^n/G_M^n - 1

- E12-09-016 in Hall A (Cates, Wojtsekhowski, Riordan).
- Double Polarization Asymmetry: Get A_{en}^V from $^3\vec{\mathrm{He}}(\vec{e}, e'n)pp$.
- Longitudinally polarized electron beam.
- $^3\mathrm{He}$ target polarized perpendicular to the momentum transfer.
- Electron arm: BigBite spectrometer.
- Neutron arm: hadron calorimeter HCal (overlap with GEp(5) and Hall A G_M^n).
- Beamtime: 50 days.
- Kinematics and Uncertainties:

Q^2 (GeV^2)	5.0	6.8	8.0
$\Delta\left[\frac{\mu G_E}{G_M}\right]_{stat}$	0.027	0.022	0.032
$\Delta\left[\frac{\mu G_E}{G_M}\right]_{syst}$	0.018	0.021	0.013

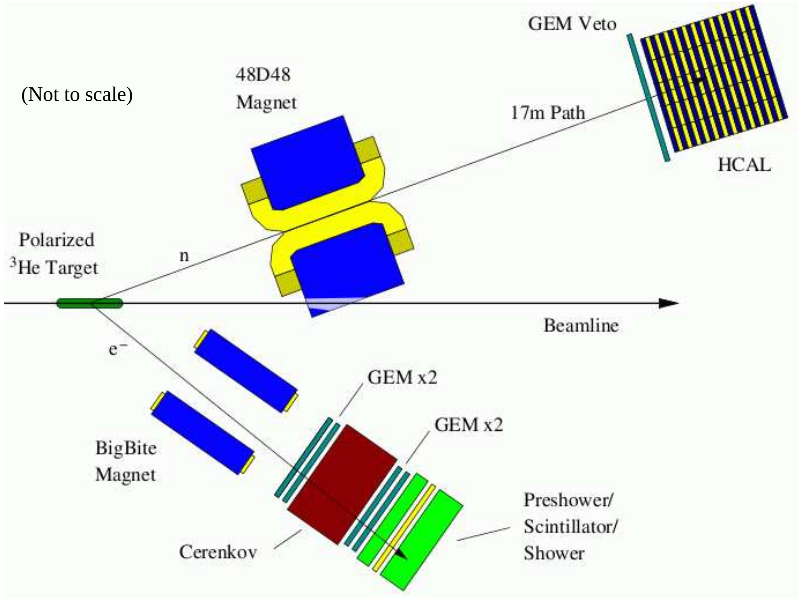

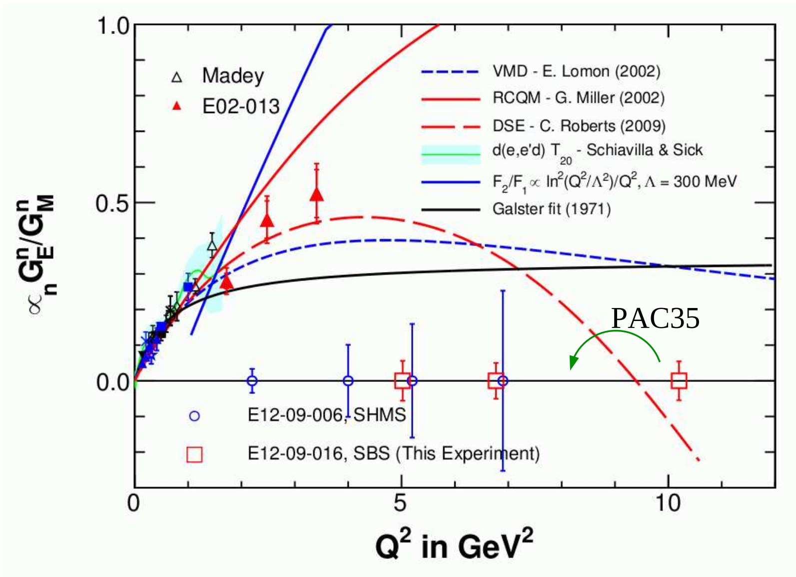

Neutron Form Factor Ratio G_E^n/G_M^n - 2

- E12-11-009 in Hall C (Anderson, Arrington, Kowalski, Madey, Plaster, Semenov).
- Polarization transfer using $^2\mathrm{H}(\vec{e}, e'\vec{n})p$:

$$\frac{G_E^n}{G_M^n} = -\frac{P_t}{P_l}\frac{E+E'}{2M}\tan\left(\frac{\theta_e}{2}\right)$$

- Electron arm: Super High Momentum Spectrometer (SHMS).
- Neutron arm: neutron polarimeter with tapered-gap neutron-spin-precession magnet and proton recoil detection.
- Kinematics: $\mathrm{Q}^2 = 3.95, 6.88\ (\mathrm{GeV/c})^2$.
- Beamtime: 50 days.
- Systematic uncertainties about 2-3%.
- Statistical uncertainties about 10-16%.
- Complementary to the $^3\mathrm{He}$ experiment.

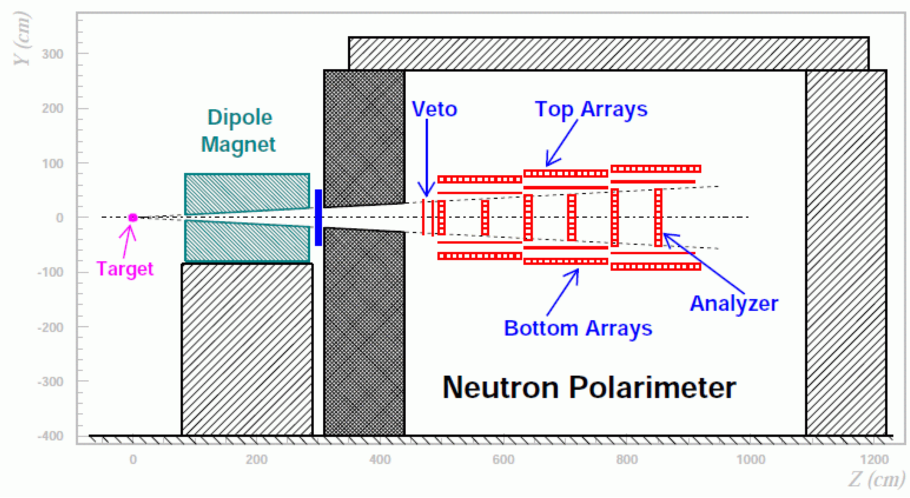

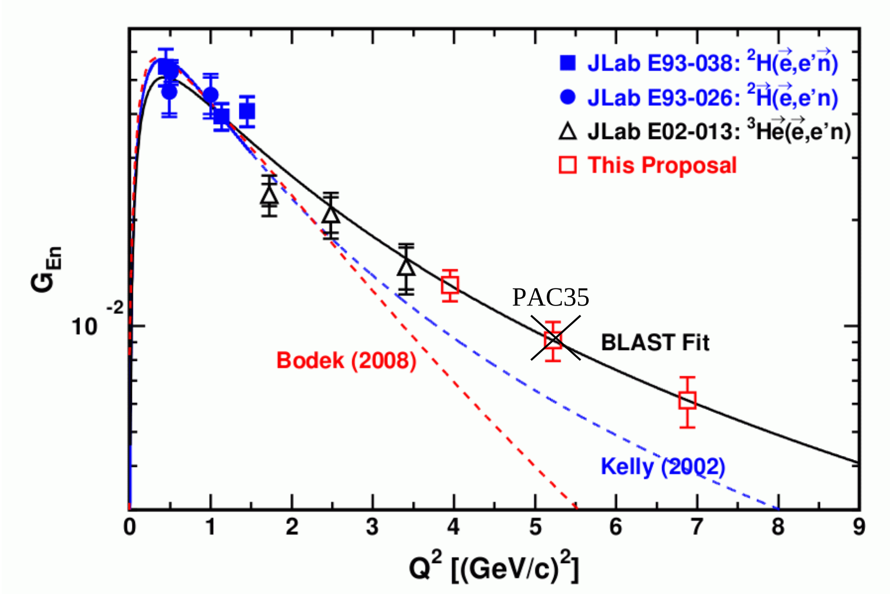

Theory Progress

The EEFFs emerge from Quantum Chromodynamics (QCD), but calculations here require non-perturbative methods.

- Vector Meson Dominance (VMD) and dispersion analyses fit all four EEFFs, but use many parameters.

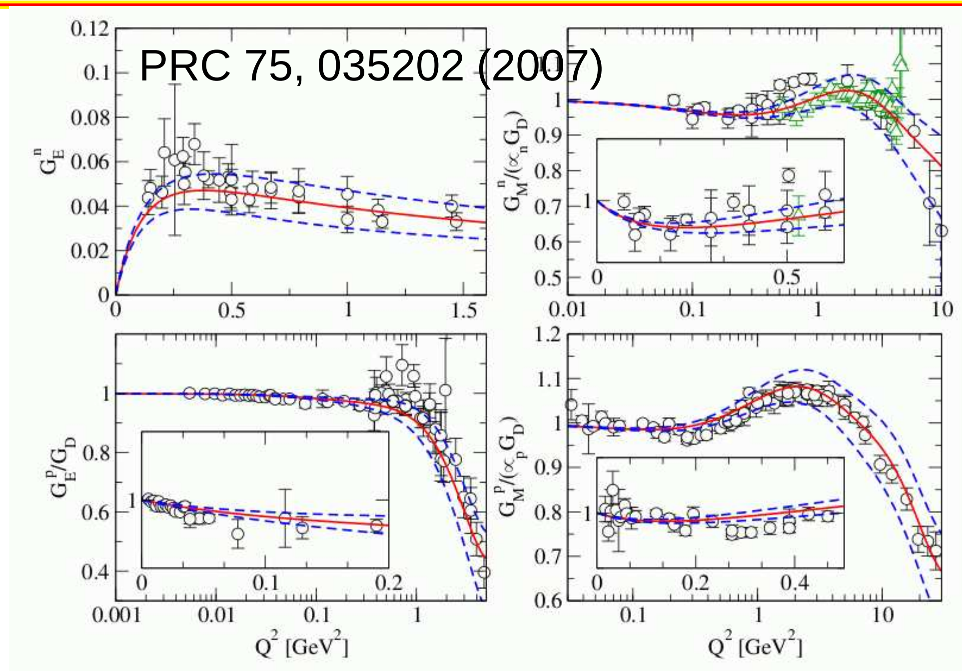

Theory Progress

The EEFFs emerge from Quantum Chromodynamics (QCD), but calculations here require non-perturbative methods.

- Vector Meson Dominance (VMD) and dispersion analyses fit all four EEFFs, but use many parameters.
- Constituent Quark Models (CQMs) highlight relativity, but don't capture all properties of QCD.
- Dyson-Schwinger calculations are built on QCD, manifestly relativistic, and use constituent quarks (including the di-quark) as degrees of freedom.

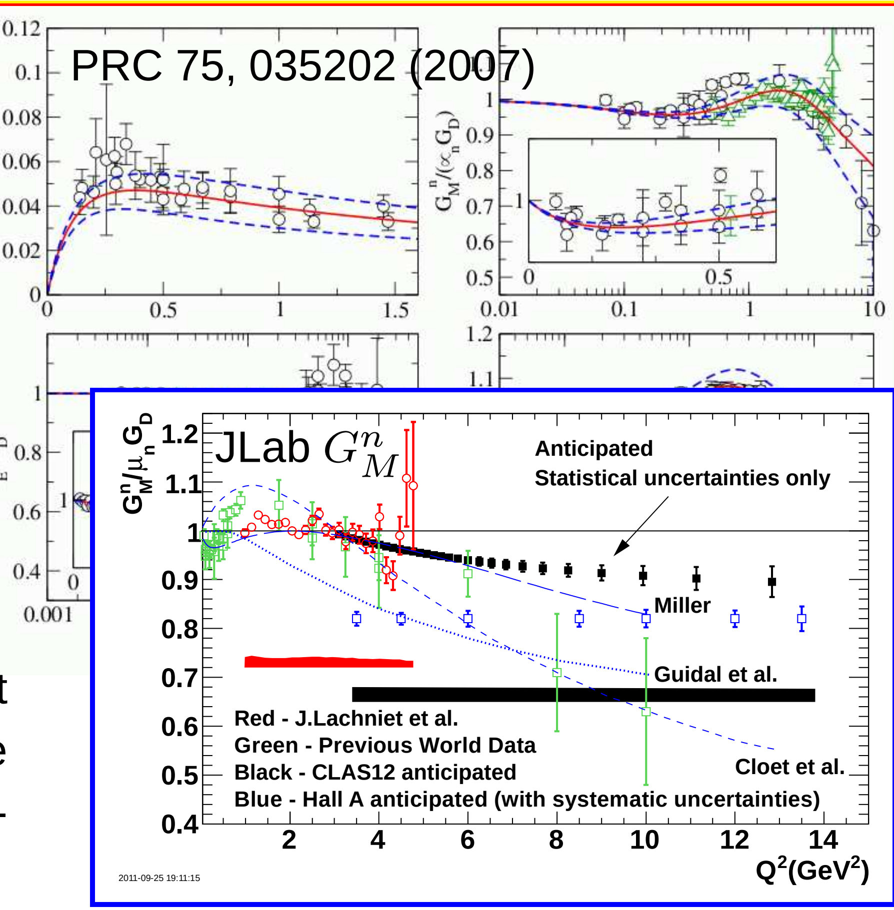

Theory Progress

The EEFFs emerge from Quantum Chromodynamics (QCD), but calculations here require non-perturbative methods.

- Vector Meson Dominance (VMD) and dispersion analyses fit all four EEFFs, but use many parameters.
- Constituent Quark Models (CQMs) highlight relativity, but don't capture all properties of QCD.
- Dyson-Schwinger calculations are built on QCD, manifestly relativistic, and use constituent quarks (including the di-quark) as degrees of freedom.
- pQCD-inspired calculations predict logarithmic scaling at high Q^2 above the range of existing data, but it is observed in the ratio F_2^p/F_1^p.

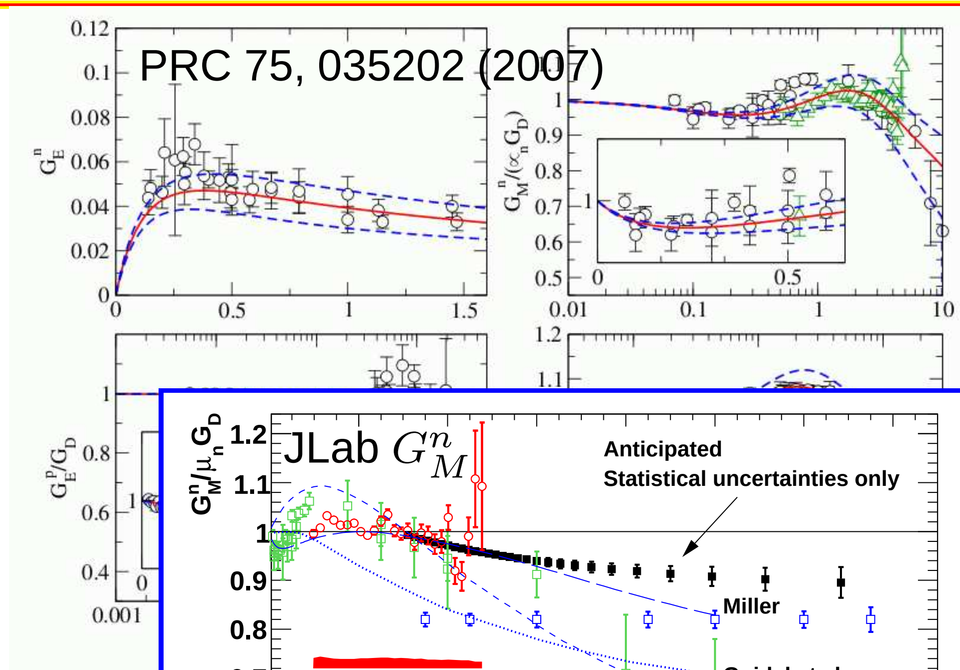

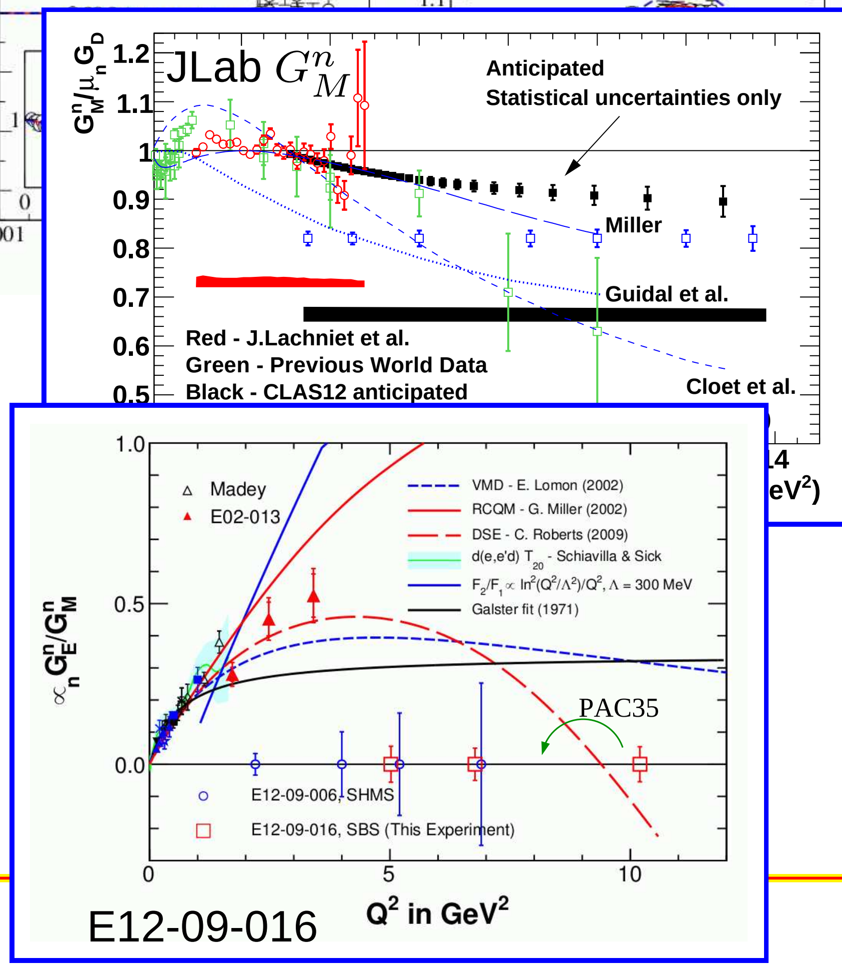

Nuclear Structure - GPDs

- Generalized Parton Distributions (GPDs) connect the valence quark distributions in transverse space and longitudinal momentum.
- EEFFs are the first moments of the GPDs and provide an important constraint.

$$\int dx \sum H^q(x,\zeta,t) = F_1(t) \quad \text{Dirac FF}$$

$$\int dx \sum E^q(x,\zeta,t) = F_2(t) \quad \text{Pauli FF}$$

- Unravel the mass $M(t)$, angular momentum $J(t)$, and force and pressure $d_1(t)$.
- Nucleon form factor measurements complement the Semi-Inclusive Deep Inelastic Scattering program.

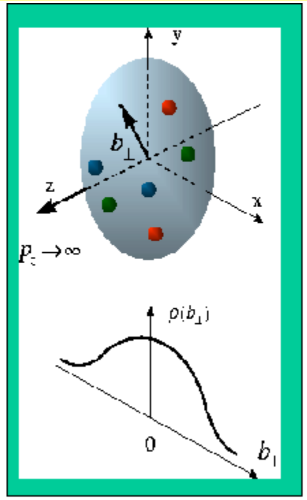

Transverse spatial distributions.

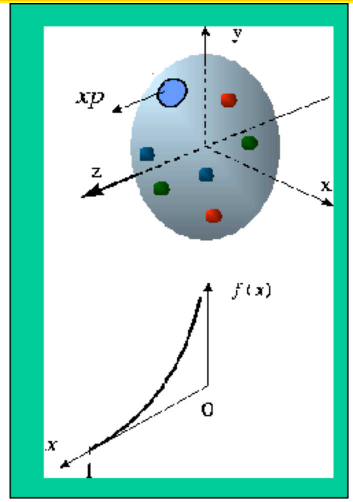

Longitudinal momentum distributions.

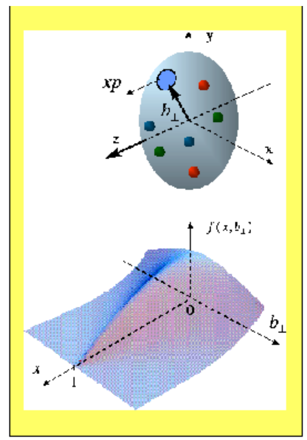

Correlated spatial and momentum distributions.

Nuclear Structure - GPDs

- Generalized Parton Distributions (GPDs) connect the valence quark distributions in transverse space and longitudinal momentum.
- EEFFs are the first moments of the GPDs and provide an important constraint

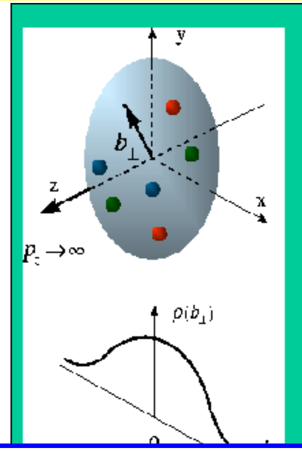

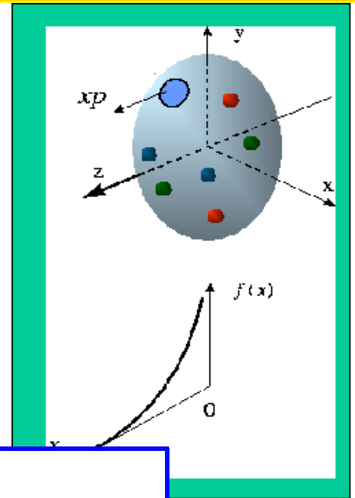

udinal
ntum
utions.

See Michel Garcon's talk on Wednesday.

$$\int dx \sum E^q(x,\zeta,t) = F_2(t)$$ Pauli FF

- Unravel the mass $M(t)$, angular momentum $J(t)$, and force and pressure $d_1(t)$.
- Nucleon form factor measurements complement the Semi-Inclusive Deep Inelastic Scattering program.

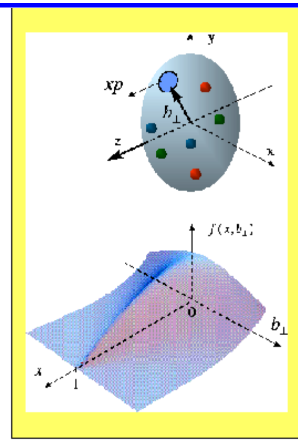

Correlated spatial and momentum distributions.

Nuclear Structure - Flavor Decomposition

- By measuring all four EEFFs we have an opportunity to unravel the contributions of the u and d quarks.
- Assume charge symmetry, no s quarks and use (Miller *et al.* Phys. Rep. **194**, 1 (1990))

$$F^u_{1(2)} = 2F^p_{1(2)} + F^n_{1(2)} \qquad F^d_{1(2)} = 2F^n_{1(2)} + F^p_{1(2)}$$

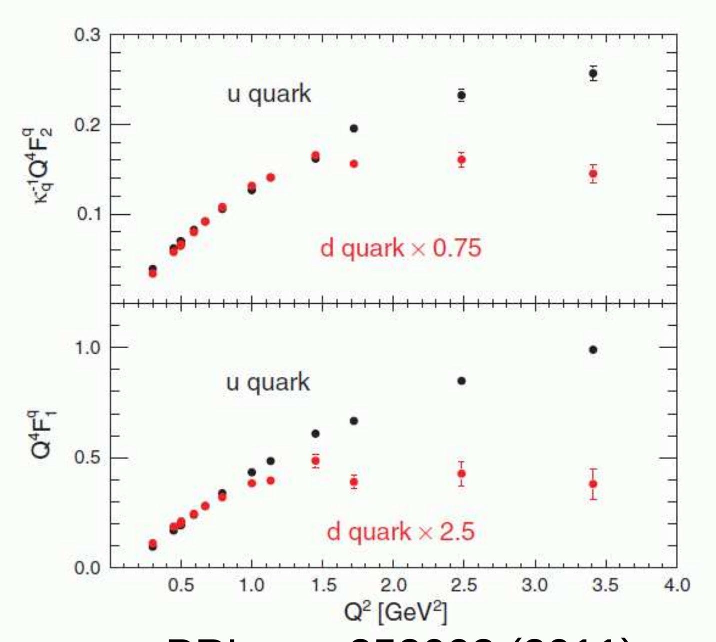

PRL **106**, 252003 (2011).

Nuclear Structure - Flavor Decomposition

- By measuring all four EEFFs we have an opportunity to unravel the contributions of the u and d quarks.
- Assume charge symmetry, no s quarks and use (Miller *et al.* Phys. Rep. **194**, 1 (1990))

$$F^u_{1(2)} = 2F^p_{1(2)} + F^n_{1(2)} \qquad F^d_{1(2)} = 2F^n_{1(2)} + F^p_{1(2)}$$

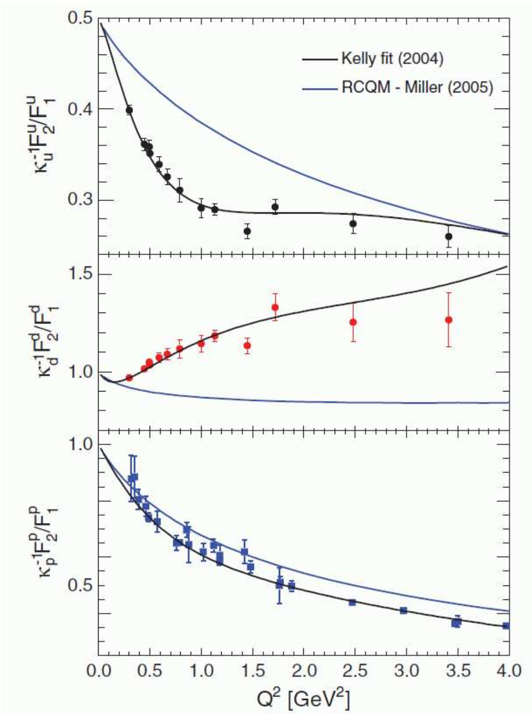

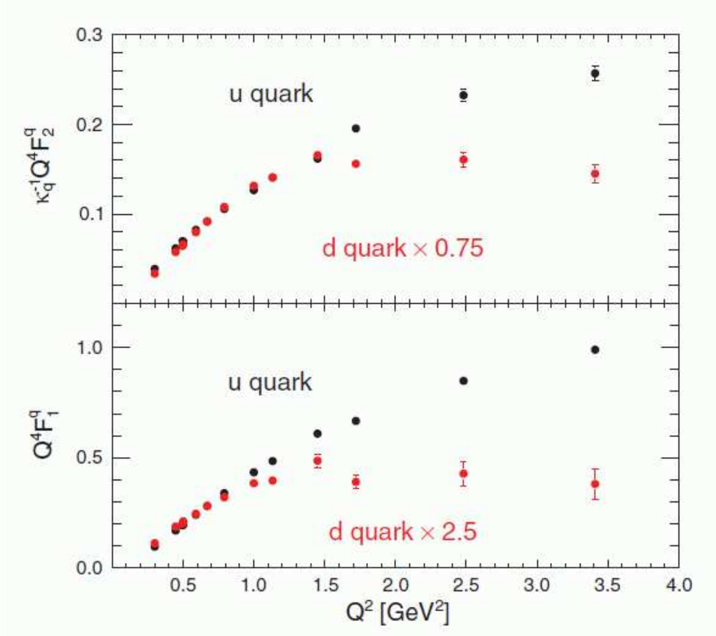

PRL **106**, 252003 (2011).

- u and d are different.
- AND different from the proton and neutron form factors.
- Evidence of di-quarks, s quark influence, ...?

Lattice QCD

- Lattice gauge theory is the only means of *ab initio* QCD calculations in the non-perturbative regime.
- Computationally challenging.
- EEFFs are an early test of lQCD.
  - The isovector form of the EEFFs is

$$F^V_{1,2} = \frac{F^p_{1,2} - F^n_{1,2}}{2}$$

where

$$F_1 = \frac{\tau G_M + G_E}{1+\tau} \qquad F_2 = \frac{G_M - G_E}{1+\tau}$$

where $\tau = Q^2/4M^2$.
  - This form of the EEFFs does not have disconnected diagrams which are computationally intensive.
- Expect EEFF calculation in the next decade.

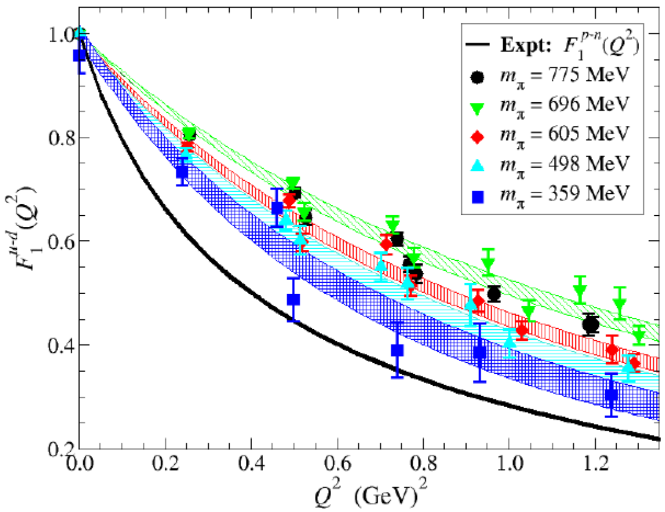

PoS **LAAT2006**, 121 (2006).

Beyond Elastic Form Factor Measurements

Additional form factor studies after the 12 GeV Upgrade.

Experiment	Spokesperson	Title	Hall	Beamtime
PR12-06-101	G. Huber	Measurement of the charged pion form factor to high Q^2	C	52 days
PR12-09-003	R. Gothe	Nucleon resonance studies with CLAS12	B	40 days

Summary and Conclusions

- Large gains over the last decade in physics understanding of the EEFFs built on new technologies and capabilities.
- Major changes in our understanding of nucleon structure.
- Jefferson Lab will mount a broad assault on the EEFFs and will significantly expand the physics reach of our understanding.
- Discovery potential in mapping out nucleon structure and understanding QCD.

Additional Slides

Jefferson Lab 12 GeV Upgrade Schedule

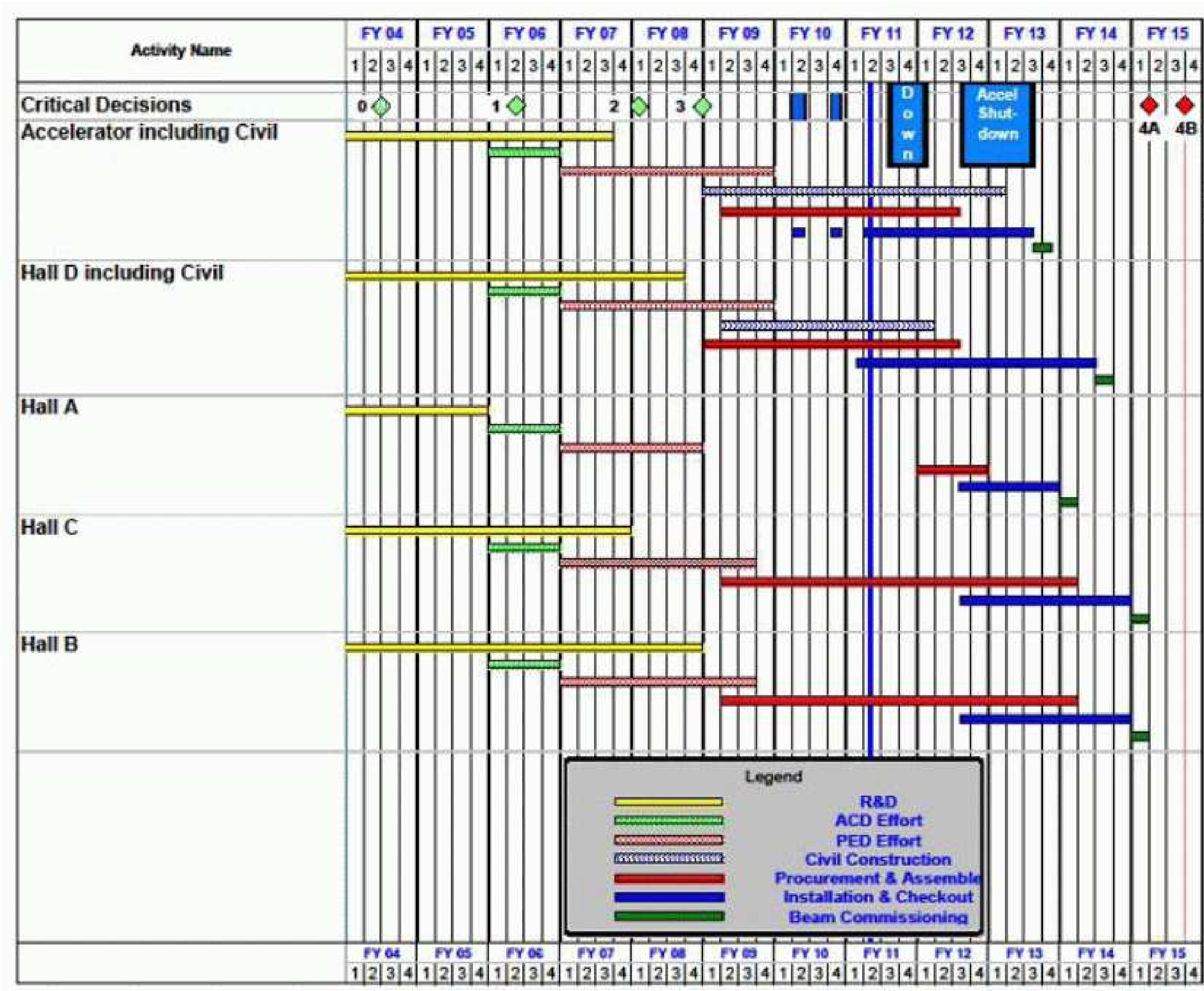

Two short parasitic installat
periods in FY10

6-month installation
May – Oct 2011

12-month installation
May 2012 – May 2013

Hall A commissioning start
October 2013

Hall D commissioning start
April 2014

Halls B/C commissioning st
October 2014

Project Completion
June 2015

Current World Data on EEFFs

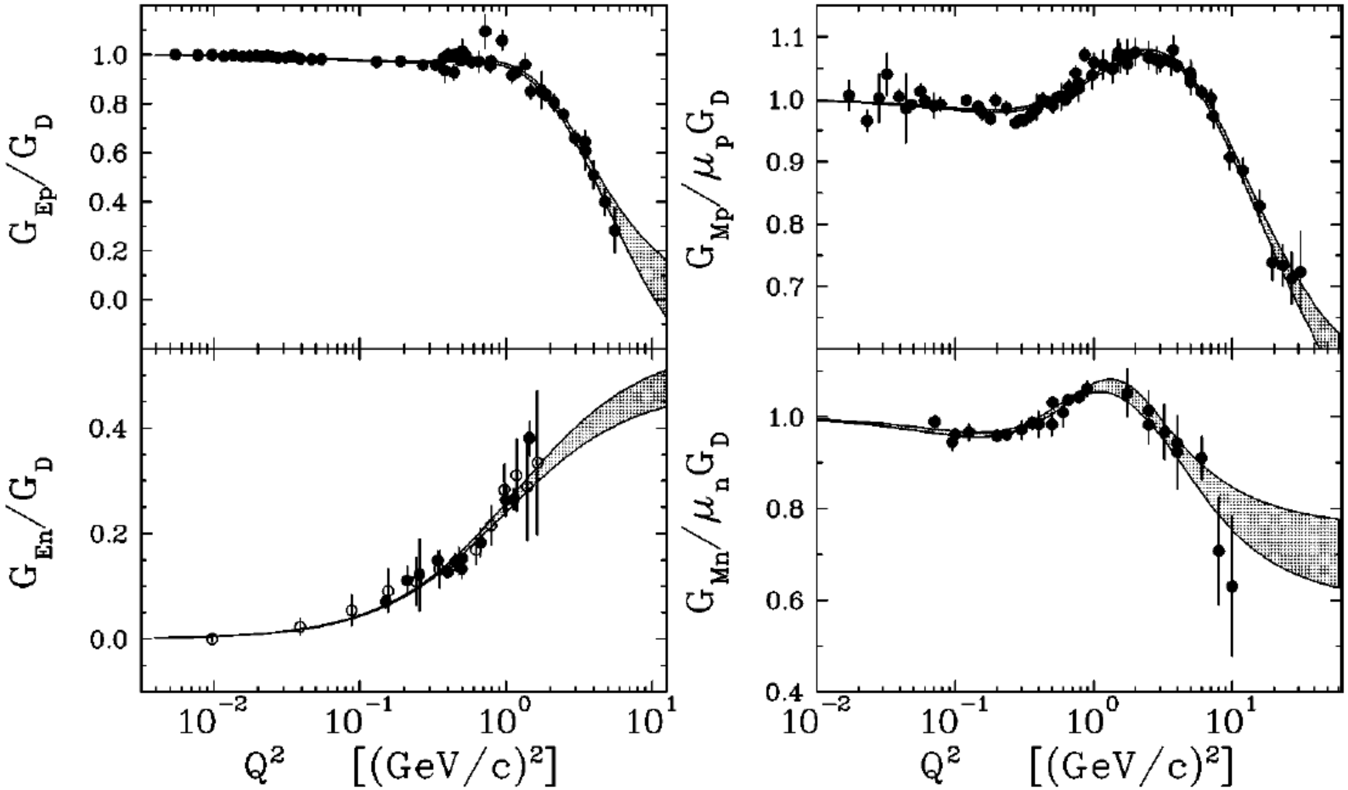

J.J.Kelly, Phys. Rev.C, 068202, 2004.

- Proton form factors have small uncertainties and reach higher Q^2.
- Neutron form factors are sparse and have large uncertainties.
- Significant deviations from the dipole form factor.

CLAS12 Detector and G_M^n Target

luminosity $\approx 10^{35}\ s^{-1} cm^{-2}$.

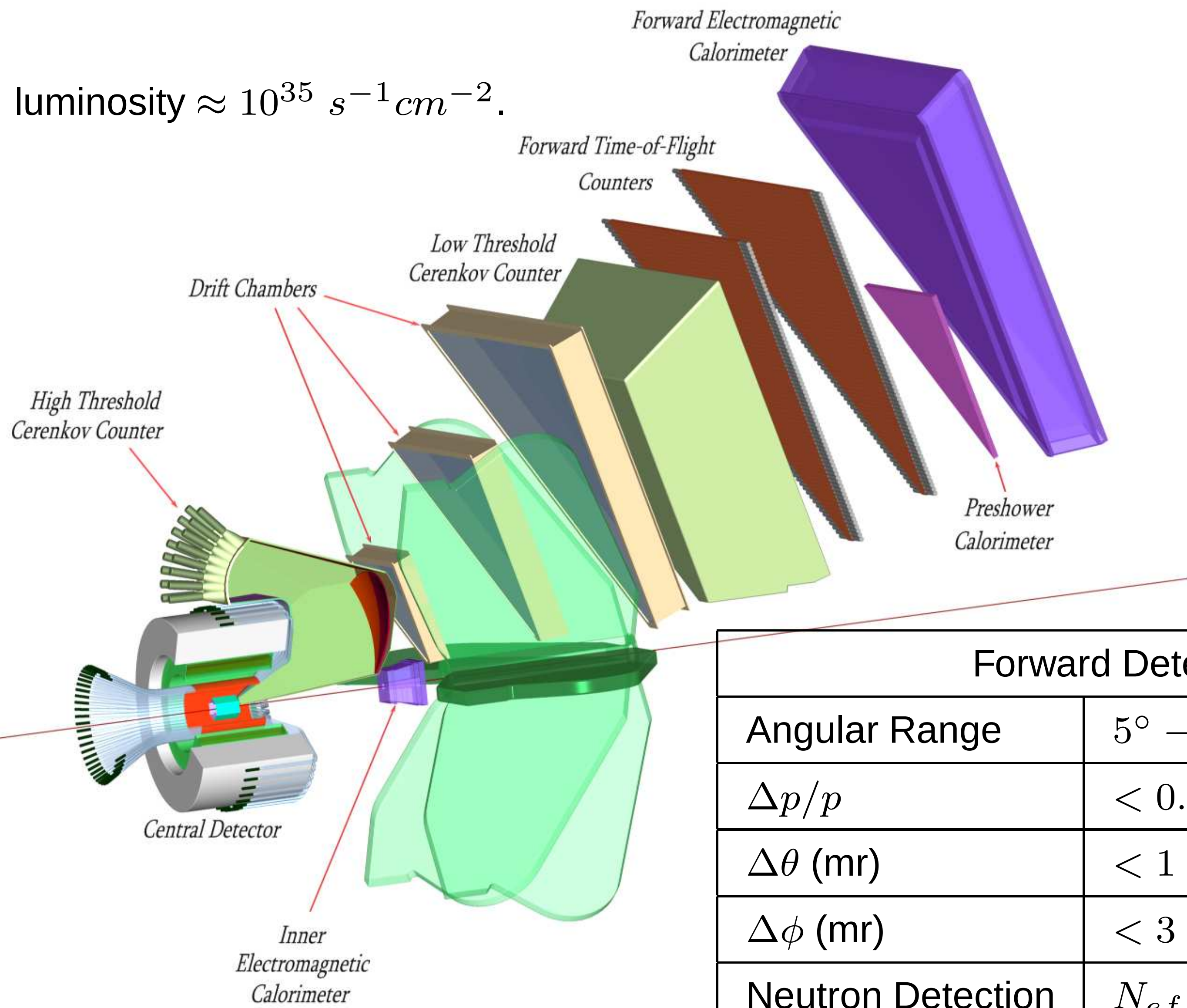

Forward Detector	
Angular Range	$5^\circ - 40^\circ$ (outbenders)
$\Delta p/p$	< 0.01 @ 5 GeV/c
$\Delta\theta$ (mr)	$< 1 \quad p > 2.5$ GeV/c
$\Delta\phi$ (mr)	$< 3 \quad p > 2.5$ GeV/c
Neutron Detection	$N_{eff} = 0.1 - 0.6$

CLAS12 Detector and G_M^n Target

luminosity $\approx 10^{35}\ s^{-1} cm^{-2}$.

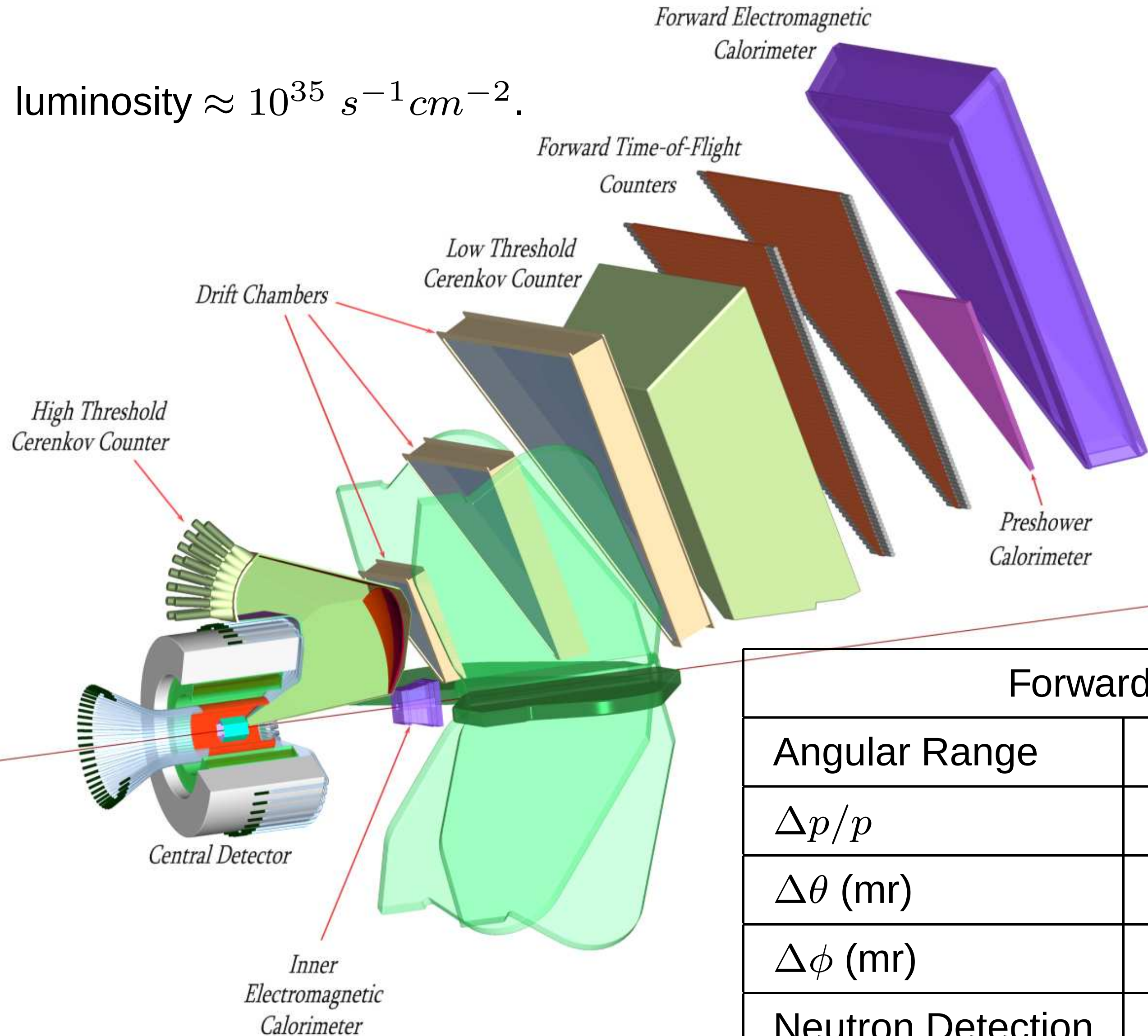

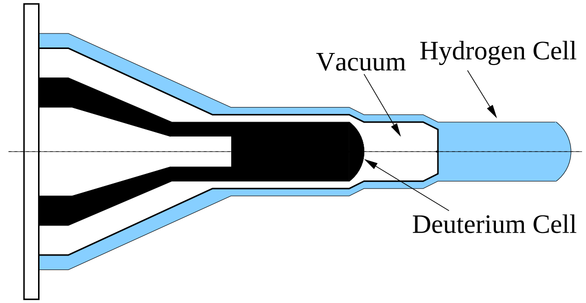

The collinear, dual, hydrogen-deuterium target enables us to collect high-precision, *in situ* calibration data so systematic uncertainties $\leq 3\%$.

Forward Detector	
Angular Range	$5^\circ - 40^\circ$ (outbenders)
$\Delta p/p$	< 0.01 @ 5 GeV/c
$\Delta\theta$ (mr)	$< 1 \quad p > 2.5$ GeV/c
$\Delta\phi$ (mr)	$< 3 \quad p > 2.5$ GeV/c
Neutron Detection	$N_{eff} = 0.1 - 0.6$

Hermiticity Cut

Challenge: Separate QE events from high-Q^2, inelastic background.

1. θ_{pq} **cut:** QE neutrons/protons emitted in a narrow cone along $\vec{q}$.
2. **Hermiticity cut:** No additional particles in the event.

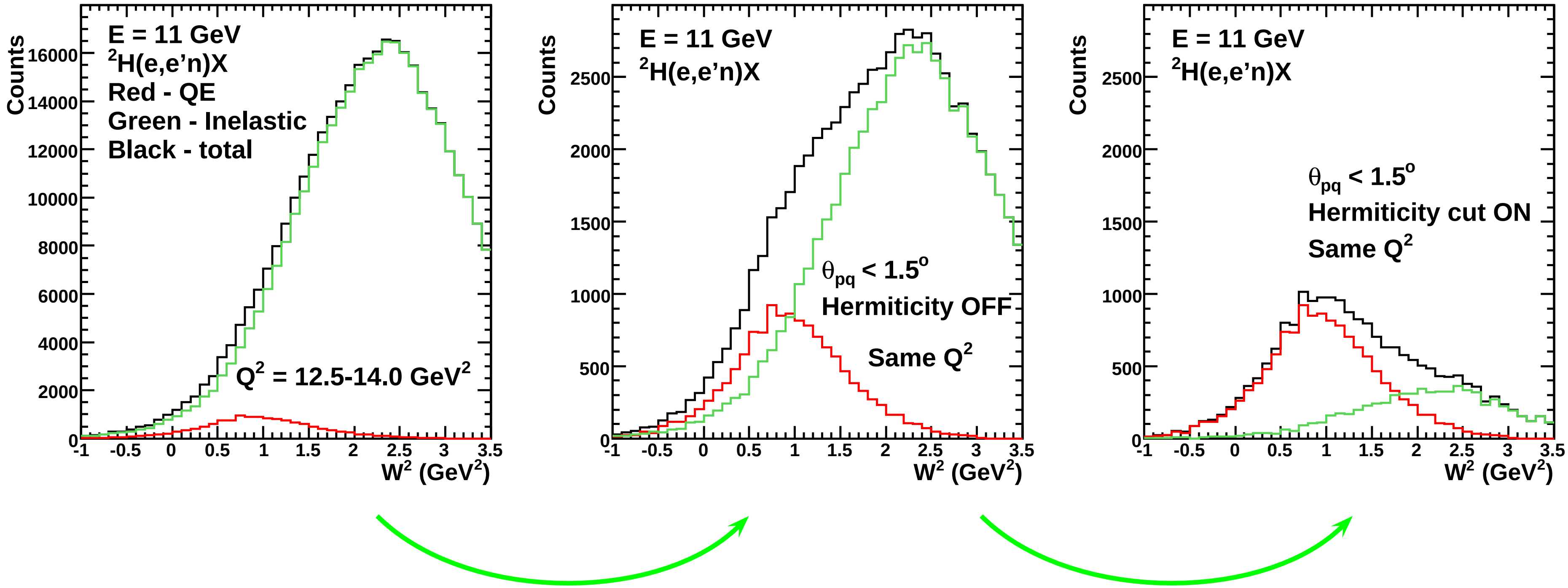

Apply θ_{pq} cut.

Apply hermiticity cut.

Calibrations - Neutron Detection Efficiency

1. Use the $ep \to e'\pi^+n$ reaction from the hydrogen target as a source of tagged neutrons in the TOF and calorimeter.
2. For electrons, use CLAS12 tracking. For π^+, use positive tracks, cut on the difference between β measured from tracking and from time-of-flight to reduce photon background.
3. For neutrons, $ep \to e'\pi^+X$ for $0.9 < m_X < 0.95\ \mathrm{GeV/c^2}$.
4. Use the predicted neutron momentum $\vec{p}_n$ to determine the location of a hit in the fiducial region and search for that neutron.
5. The CLAS6 G_M^n results.
6. GSIM12 simulation results for CLAS12 are shown in the inset. Proposed measurement will extend to higher momentum where the efficiency is stable.

Calorimeter efficiency

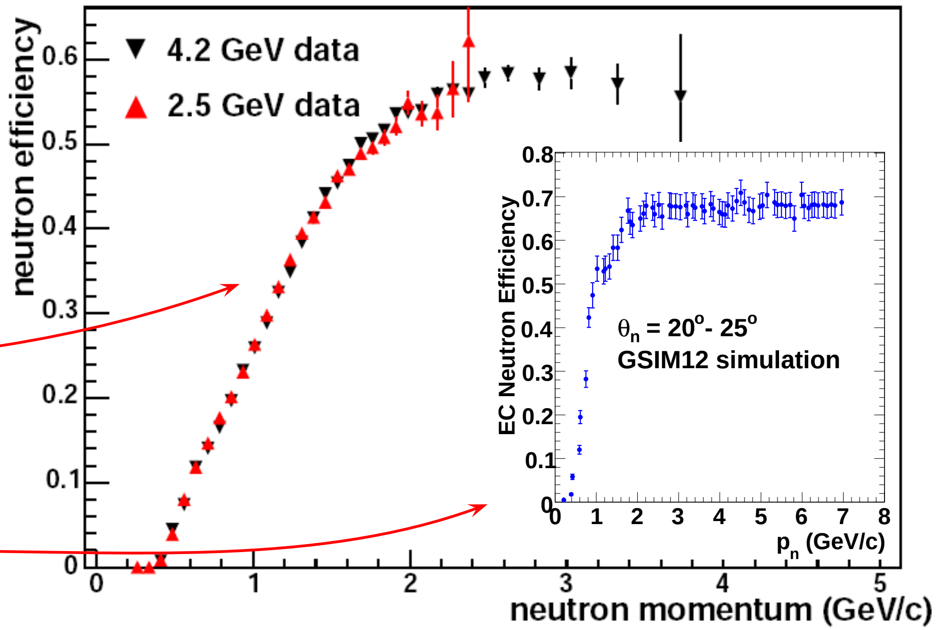

Simultaneous, *in situ* calibrations with dual hydrogen-deuterium target.

The Ratio Method - Systematic Errors

- G^n_M is related to the $e-n/e-p$ by the following (neutron (n) and proton (p)).

$$G^n_M = \pm\sqrt{\left[R\left(\frac{\sigma^p_{mott}}{\sigma^n_{mott}}\right)\left(\frac{1+\tau_n}{1+\tau_p}\right)\left({G^p_E}^2 + \frac{\tau_p}{\varepsilon_p}{G^p_M}^2\right) - {G^n_E}^2\right]\frac{\varepsilon_n}{\tau_n}}$$

- Upper limits on systematic error from the CLAS6 measurement ($\Delta G^n_M/G^n_M = 2.7\%$).

Quantity	$\delta G^n_M/G^n_M \times 100$	Quantity	$\delta G^n_M/G^n_M \times 100$
Neutron efficiency parameterization	< 1.5	θ_{pq} cut	< 1.0
proton σ	< 1.5	G^n_E	< 0.7
neutron accidentals	< 0.3	Neutron MM cut	< 0.5
neutron proximity cut	< 0.2	proton efficiency	< 0.4
Fermi loss correction	< 0.9	Radiative corrections	< 0.06
Nuclear Corrections	< 0.2		

- CLAS12 Goal: **$\leq$3% systematic uncertainty**

Statistical Uncertainties

- Use Alberico *et al.* (PRC 79, 065204 (2009)) to estimate G_M^n.
- $Q^2 = 3.5 - 15.0\ \mathrm{GeV}^2$, but statistical uncertainty exceeds systematic uncertainty at highest Q^2.
- Statistical Uncertainty: less than 3% for $Q^2 \approx 11.5\ \mathrm{GeV}^2$; much better at lower Q^2.
- Systematic Uncertainty: less than 3% across the full Q^2 range.

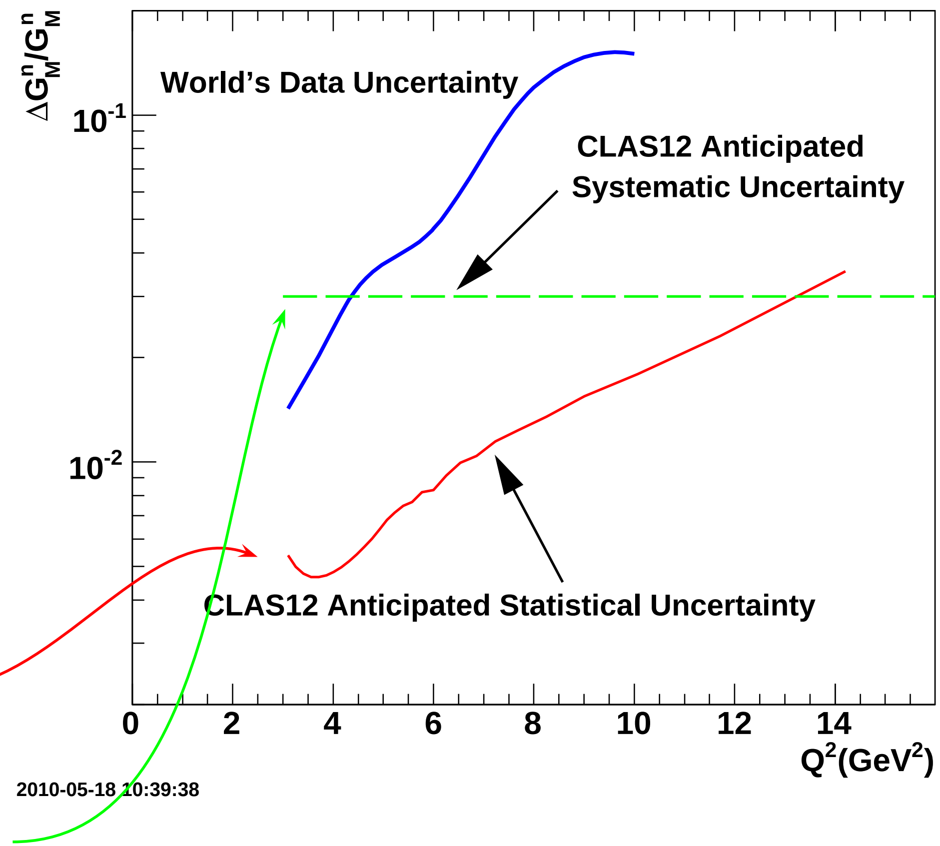

Statistical Uncertainties

- Use Alberico *et al.* (PRC 79, 065204 (2009)) to estimate G_M^n.
- $Q^2 = 3.5 - 15.0\ \mathrm{GeV}^2$, but statistical uncertainty exceeds systematic uncertainty at highest Q^2.
- Statistical Uncertainty: less than 3% for $Q^2 \approx 11.5\ \mathrm{GeV}^2$; much better at lower Q^2.
- Systematic Uncertainty: less than 3% across the full Q^2 range.

Will extend the Q^2 range of G_M^n with higher precision.

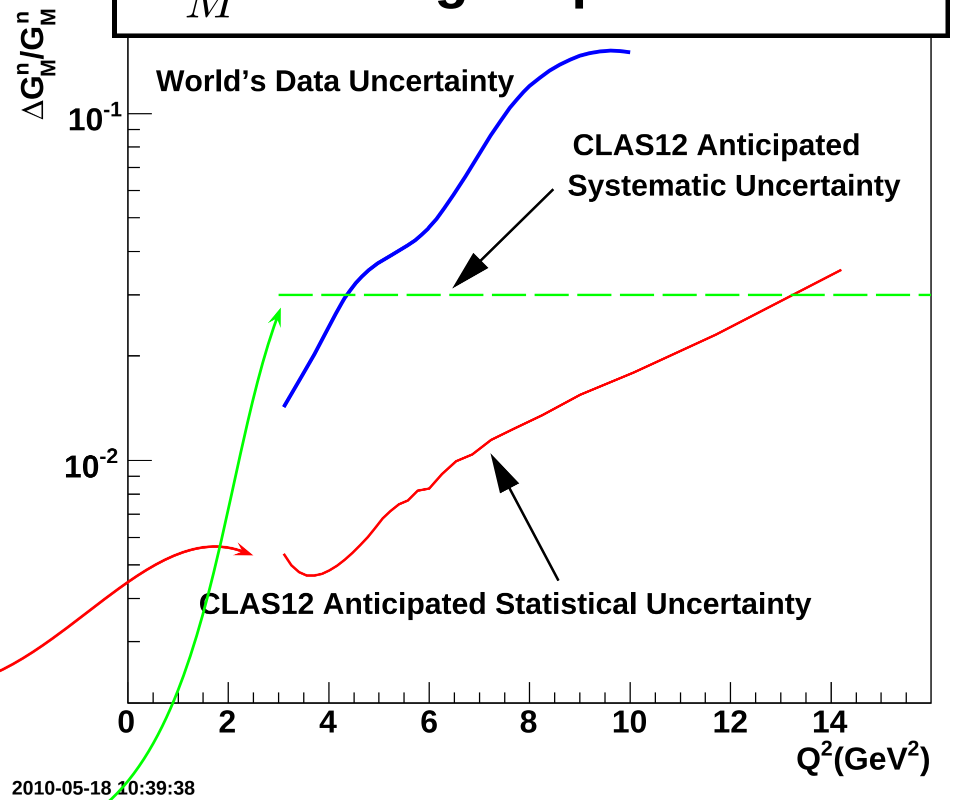

Approved for 30 days of running, A$^-$ rating.

More on the CLAS12 Detector

	Forward Detector	Central Detector
Angular Range		
Charged Particles	$5^\circ - 40^\circ$	$40^\circ - 135^\circ$
Photons	$2^\circ - 40^\circ$	N/A
Resolution		
$\Delta p/p$	< 0.01 @ 5 GeV/c	< 0.03 @ 0.5 GeV/c
$\Delta\theta$ (mr)	< 0.5	< 10
$\Delta\phi$ (mr)	< 0.5	< 6
Neutron Detection		
N_{eff}	0.1-0.6	0.1

Update for E12-07-104: Comparison of CLAS12 and E12-09-019 methods

1. To reduce inelastic background further, reduce the maximum θ_{pq}.

$f_{IN} = \frac{inelastic}{total}$ for $W^2 < 1.2\ \mathrm{GeV}^2$.

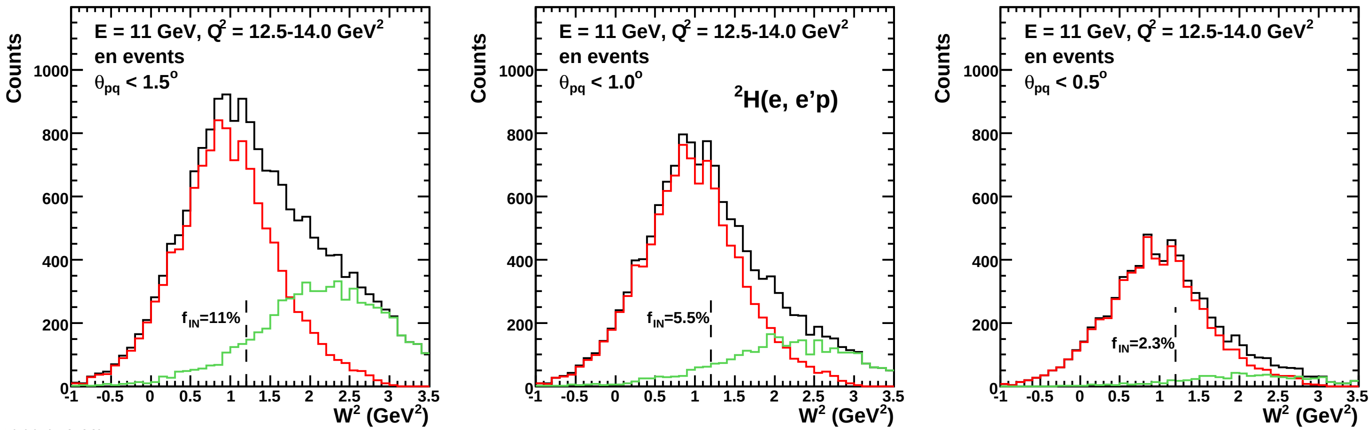

2. In a similar Q^2 range, in E12-09-019 only the θ_{pq} cut will be used leaving more inelastic background contaminating the the QE peak.

3. At higher Q^2 (*i.e.* in PR10-005), the width of the inelastic component will continue to increase.